Lymphoblastic Leukemia/Lymphoma

9

Qian-Yun Zhang

Lymphoblastic leukemia/lymphoma (i.e., acute lymphoblastic leukemia/lymphoma or ALL) is the most common type of cancer in childhood. The age-adjusted incidence rate is 3.1/100,000 in children, so approximately 2500–3000 children are diagnosed with acute lymphoblastic leukemia (ALL) each year in the United States). Approximately 80–85% of the cases are B-ALL and 10–15% are T-ALL (Table 9.1). Approximately 75% of ALL occurs in children under 6 years old, but it can occur at any age [1, 2]. Genetic factors play important roles in cancer initiation. ALL with t(12;21) *ETV6-RUNX1* fusion is found in newborn blood spots from Guthrie cards in patients who developed ALL later. Patients with Down syndrome have an increased risk for ALL, and twins and siblings of ALL patients also have an increased incidence of ALL [3]. Other factors that may contribute to the risk of developing ALL include radiation exposure, increased maternal age, male sex, and Caucasian race. Patients typically present with anemia, thrombocytopenia, and/or neutropenia-related signs and symptoms such as fatigue, weakness, shortness of breath, easy bruising, bleeding, and infection. A typical diagnostic workup for ALL patients is listed in Tables 9.2 and 9.3, with findings illustrated in Figs. 9.1, 9.2, 9.3, 9.4, 9.5, 9.6, 9.7, 9.8, 9.9, 9.10, 9.11, 9.12, 9.13, 9.14, 9.15, 9.16, 9.17, 9.18, 9.19, 9.20, 9.21, 9.22, 9.23, 9.24, 9.25, 9.26, 9.27, 9.28, 9.29, 9.30, 9.31, 9.32, 9.33, 9.34, 9.35, and 9.36.

Although ALL is primarily a disease of blood and bone marrow, some patients may present with extramedullary disease and have less than 25% blasts in the marrow; those patients meet criteria for lymphoblastic lymphoma (LBL). The definition of acute lymphoblastic leukemia (ALL) requires greater than 25% of blasts in the bone marrow, but this definition is arbitrary. ALL and LBL are biologically similar but differ in their clinical manifestations; they are collectively called ALL. Both B-ALL and T-ALL may exhibit a spectrum of maturation. Tables 9.4 and 9.5 summarize the immunophenotypic characteristics of the different stages.

The prognosis of ALL depends on clinical features, laboratory findings, genetic aberrations, and responsiveness to chemotherapy (Tables 9.6, 9.7, and 9.8 and Figs. 9.37, 9.38, and 9.39) [2, 4–6]. The overall complete remission rate in children is greater than 95% but it is much lower (60–85%) in adults. The survival rate is greater than 90% in children, 40% for ages 25 to 59 years, and less than 20% in older patients [7–10].

Q.-Y. Zhang (✉)
Department of Pathology, University of New Mexico,
Albuquerque, NM, USA
e-mail: qzhang@salud.unm.edu

T.I. George, D.A. Arber (eds.), *Atlas of Bone Marrow Pathology*, Atlas of Anatomic Pathology,
https://doi.org/10.1007/978-1-4939-7469-6_9

Table 9.1 2017 WHO classification of ALL

B-lymphoblastic leukemia/lymphoma, NOS
B-lymphoblastic leukemia/lymphoma with t(9;22)(q34.1;q11.2); *BCR-ABL1*
B-lymphoblastic leukemia/lymphoma with t(v;11q23.3); *KMT2A* rearranged
B-lymphoblastic leukemia/lymphoma with t(12;21)(p13.2;q22.1); *ETV6-RUNX1*
B-lymphoblastic leukemia/lymphoma with hyperdiploidy
B-lymphoblastic leukemia/lymphoma with hypodiploidy (hypodiploid ALL)
B-lymphoblastic leukemia/lymphoma with t(5;14)(q31.1;q32.3); *IL3-IGH*
B-lymphoblastic leukemia/lymphoma with t(1;19)(q23;p13.3); *TCF3-PBX1*
B-lymphoblastic leukemia/lymphoma, *BCR-ABL1–like*
B-lymphoblastic leukemia/lymphoma with *iAMP21*
T-lymphoblastic leukemia/lymphoma
Early T-cell precursor lymphoblastic leukemia
Provisional entity: Natural killer (NK) cell lymphoblastic leukemia/lymphoma

Table 9.2 Common tests recommended at the diagnosis and follow-up of ALL

Tests	When to do	Value of the test
Complete blood count	At diagnosis and follow-up	For diagnosis and to assess hematopoiesis
Bone marrow aspiration and core biopsy	At diagnosis and follow-up	For diagnosis and to assess residual disease and hematopoiesis
Flow cytometric study	At diagnosis and optional at follow-up	To detect leukemic cells and to monitor minimal residual disease
COG FISH panel in pediatric patients	At diagnosis and optional at follow-up	For prognosis and monitoring if there is established abnormality
Cytogenetic analysis	At diagnosis and optional at follow-up	For prognosis, for monitoring if there is established abnormality, for detection of clonal evolution
Molecular study for *BCR-ABL1* fusion	At diagnosis and follow-up	For monitoring
Ph-like workup[a]	At diagnosis	For prognosis
Metabolic panel	At diagnosis and optional at follow-up	To assess physiological status
Tumor lysis syndrome workup	At diagnosis and optional at follow-up	To assess the presence and severity of tumor lysis syndrome
Cerebrospinal fluid	At diagnosis and follow-up	For prognosis and monitoring
Radiographic study	At diagnosis, optional	To assess extramedullary involvement

COG Children's Oncology Group; *FISH* fluorescence in situ hybridization
[a]Ph-like (*BCR-ABL1*-like): ALL with gene expression profile similar to Ph + ALL but without *BCR-ABL1* fusion

Table 9.3 Bone marrow staging at follow-up; cerebrospinal fluid staging

BM stages	*BM findings*
M1 marrow	<5% blasts
M2 marrow	5% to <25% blasts
M3 marrow	≥25% of blasts
CSF stages	*CSF findings*
CNS1	No detectable leukemia cells in the CSF
CNS2	<5 white blood cells per microliter of blood and a positive cytospin preparation for blasts
CNS3	>5 white blood cells per microliter and a positive cytospin

BM bone marrow; *CSF* cerebrospinal fluid

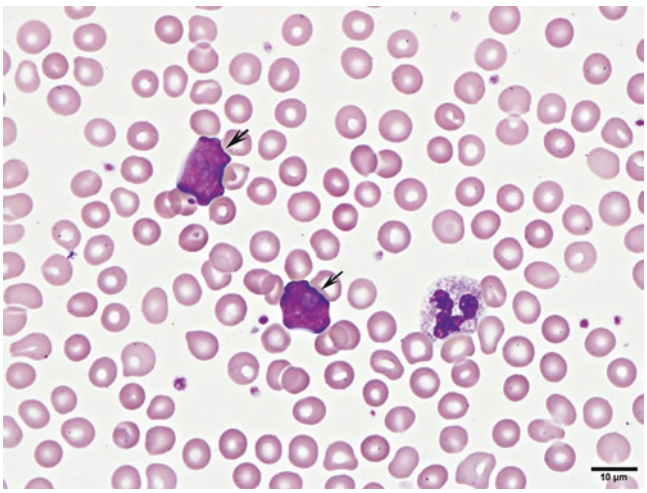

Fig. 9.1 A complete blood count (CBC) is an essential part of the workup for acute lymphoblastic leukemia/lymphoma (ALL) (Table 9.2). Peripheral blood smear review often reveals circulating blasts. This peripheral blood from a 5-month-old boy with a recent diagnosis of B-lymphoblastic leukemia shows two blasts and a neutrophil. The blasts are small to intermediate in size and have scant blue cytoplasm, fine to slightly clumped chromatin, and one or two prominent nucleoli. Scattered platelets are seen in the background. When caught early, the patient may not have peripheral blood cytopenias, such as in this case, but most patients will present with cytopenia-related signs and symptoms such as fatigue, weakness, dizziness, or shortness of breath secondary to anemia; infection secondary to neutropenia; bleeding or bruising secondary to thrombocytopenia; pain in arms, legs, or joints due to leukemic cell infiltrate; and systemic symptoms such as unexplained weight loss

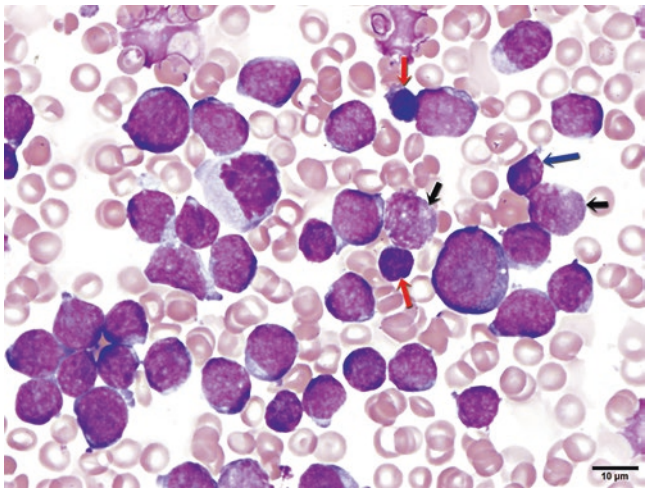

Fig. 9.3 Typically the bone marrow aspirate reveals predominantly lymphoblasts of variable size ranging from small to large. Normal hematopoietic elements are markedly reduced. In this image, a lonely erythroid precursor (red arrow), two myelocytes (black arrows), and two lymphocytes (blue arrows) are admixed with lymphoblasts

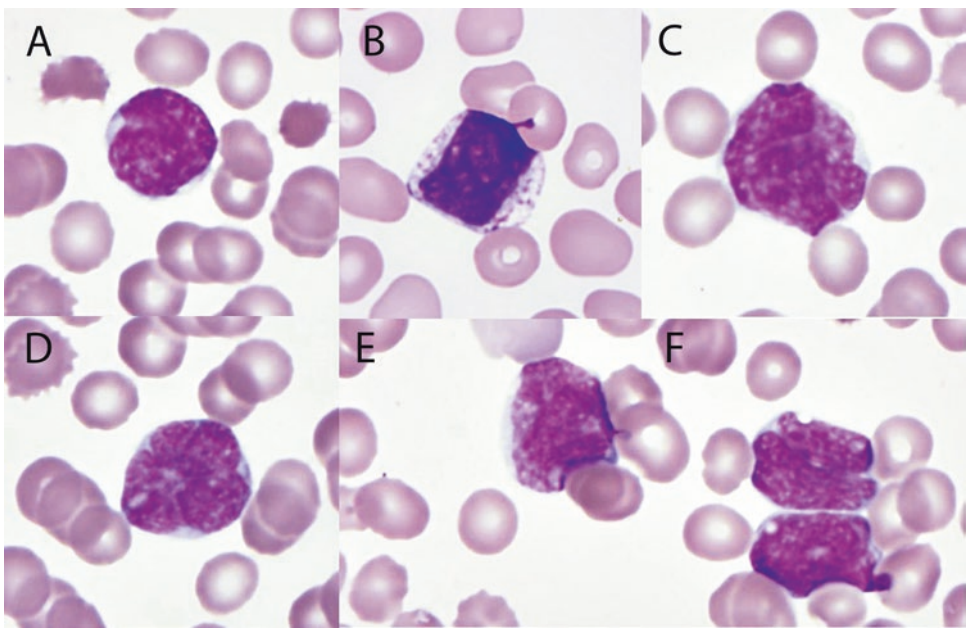

Fig. 9.2 ALL blasts can exhibit various morphology, such as seen in this composite image. The blasts can range from small to large in size. The nuclei can be round or slightly cleaved (**a**). Most blasts have scant blue cytoplasm, but rarely the blast can have moderately abundant cytoplasm with coarse azurophilic granules (**b**). Blasts can have deeply cleaved nuclei (**c**,**e**,**f**) or flower-shaped nuclei (**d**)

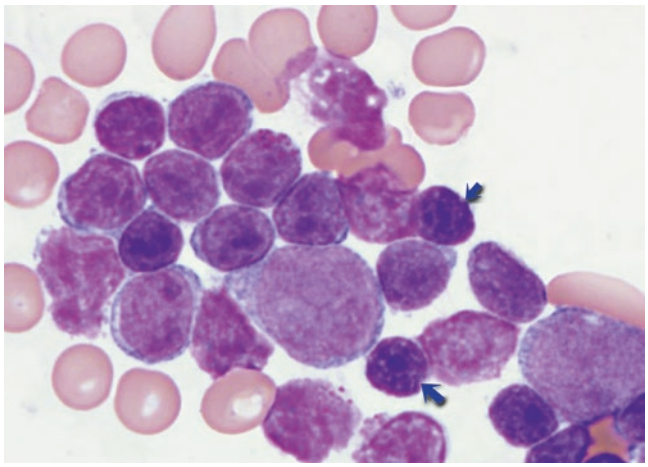

Fig. 9.4 Higher-power view of the bone marrow aspirate reveals lymphoblasts with slightly clumped chromatin pattern in the small blasts, to open and fine chromatin in the large blasts. In comparison, two small mature lymphocytes (blue arrows) are also present

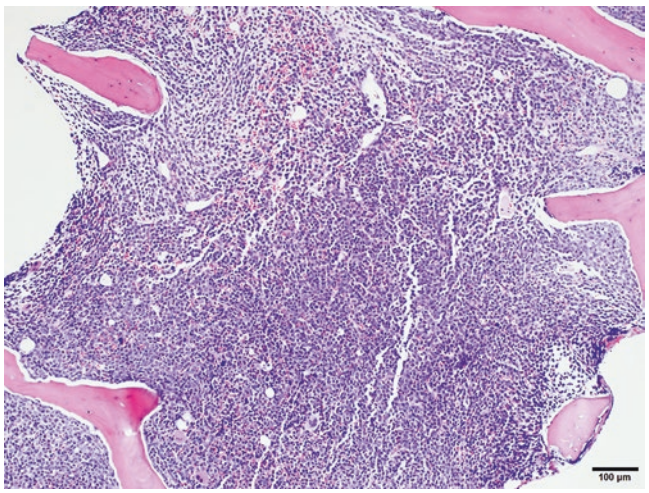

Fig. 9.5 Low-power view of a bone marrow core biopsy shows that the marrow is diffusely replaced by lymphoblasts. Admixed is markedly reduced trilineage hematopoiesis. Rare megakaryocytes can be seen at this low power

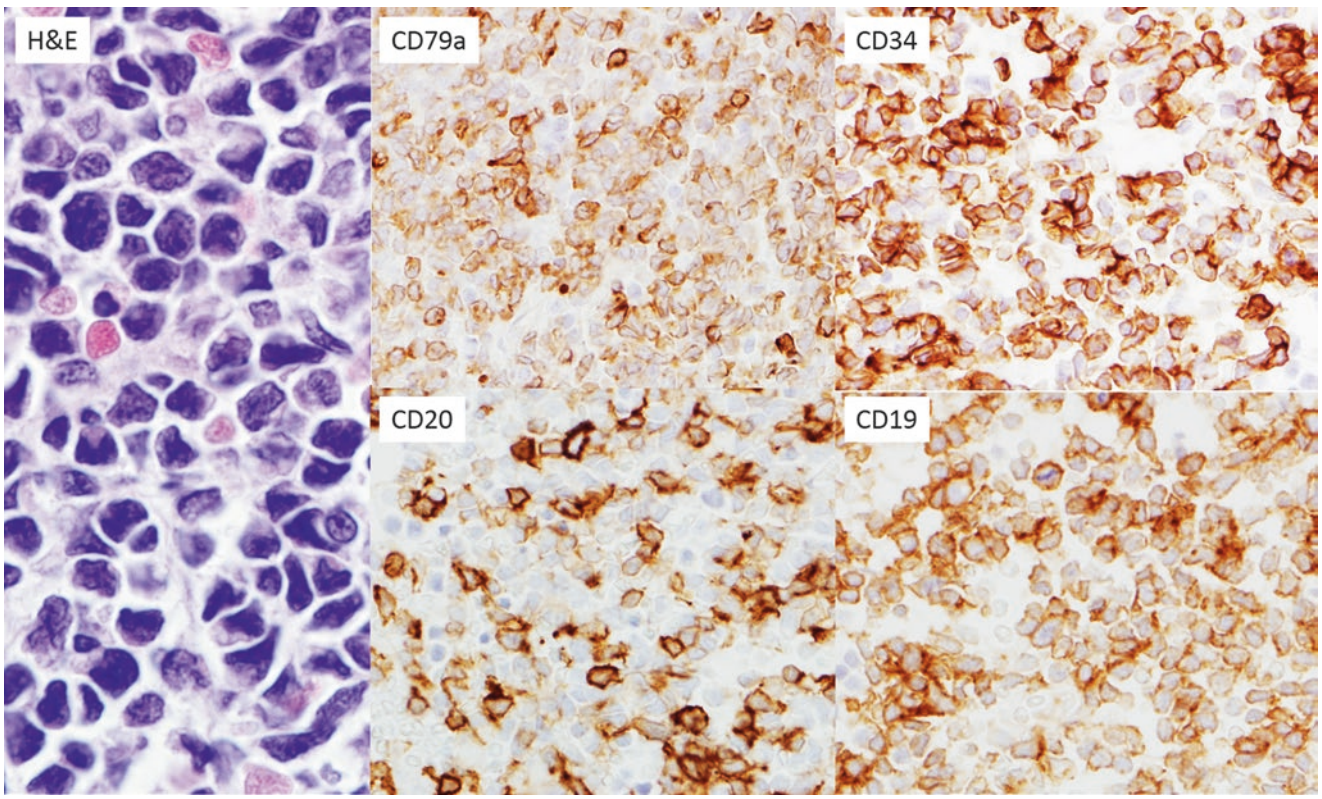

Fig. 9.6 High-power view of the bone marrow core biopsy demonstrates the lymphoblasts in detail. The blasts exhibit variation in size and have condensed to open chromatin, round to deeply cleaved nuclear contours, and inconspicuous to prominent nucleoli. Immunohistochemical stains demonstrate that the blasts express CD79a, CD34, and CD19, and a subset of cells also express CD20

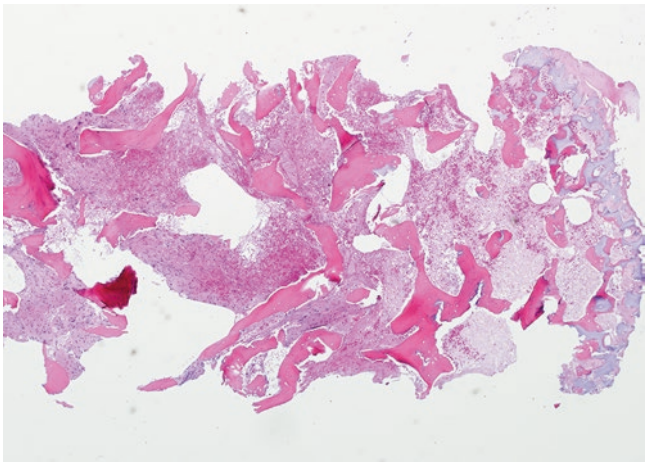

Fig. 9.7 Rarely, the marrow can be necrotic. As shown in this case, the marrow is completely necrotic, and the immunophenotype by both flow cytometry and immunohistochemical stains failed to establish the diagnosis. There were no circulating blasts in the peripheral blood. The patient had to undergo repeated bone marrow biopsy to finally reach the diagnosis of B-ALL

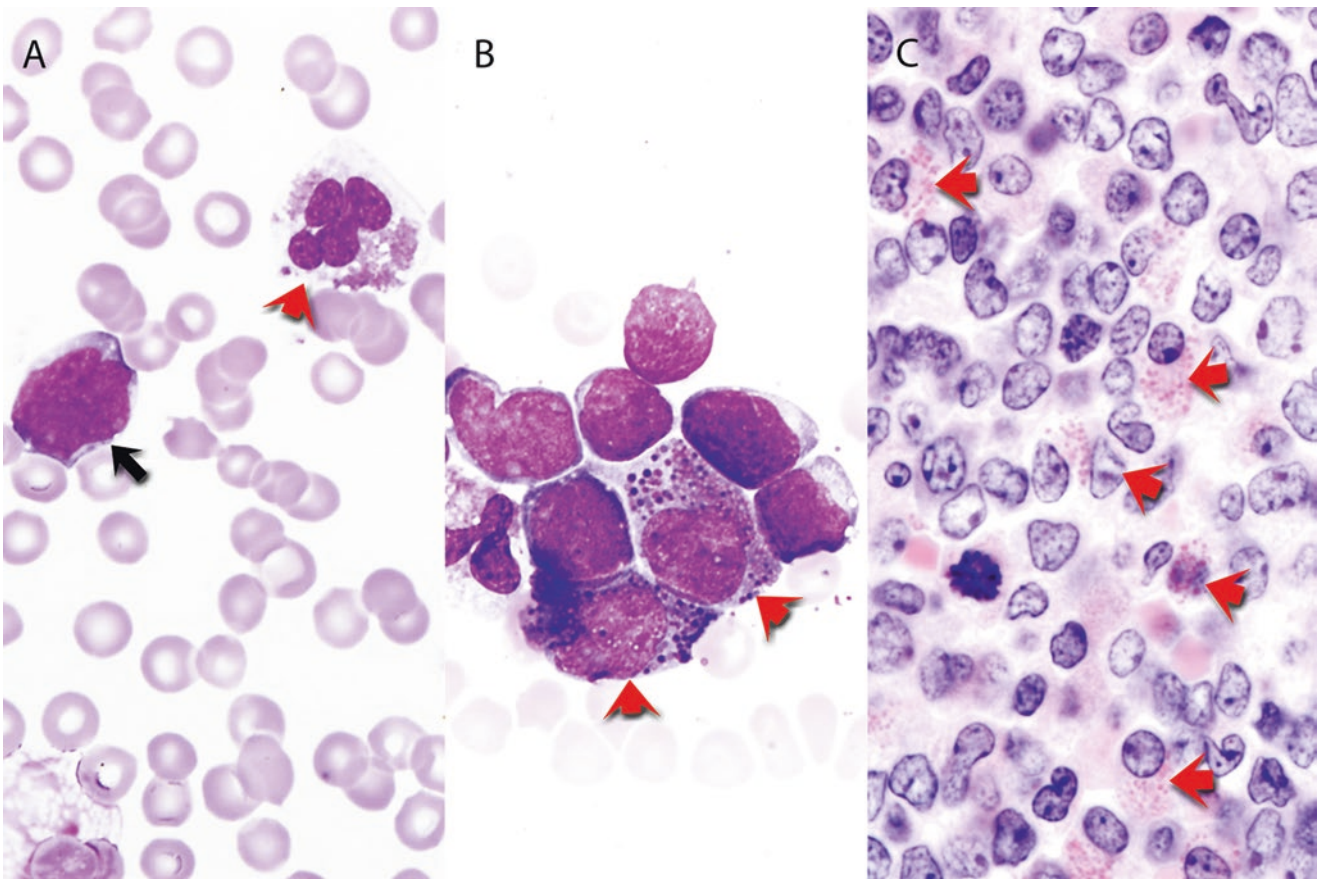

Fig. 9.8 (**a**) This patient had significant absolute eosinophilia in the peripheral blood (red arrow) in addition to circulating blasts (black arrow). (b) In the bone marrow aspirate, there were markedly increased eosinophilic precursors with mixed, coarse eosinophilic and basophilic granules (red arrows). (c) The bone marrow core biopsy showed the presence of numerous lymphoblasts with admixed eosinophilic precursors (red arrows). Cytogenetic study revealed translocation t(5;14) (q31;q32) *IL3-IGH*. This translocation involves the *IL3* gene and *IGH* gene, resulting in constitutive overexpression of the *IL3* gene, which leads to reactive eosinophilia. The eosinophils are not part of the neoplastic clone. The clinical aspects, blast morphology, and prognosis are no different from those of other types of B-ALL. The caveat regarding this type of B-ALL is that the patient may present with eosinophilia without circulating blasts. Therefore, a high index of suspicion is required in patients with eosinophilia without an apparent etiology. Bone marrow biopsy may be required to establish the diagnosis

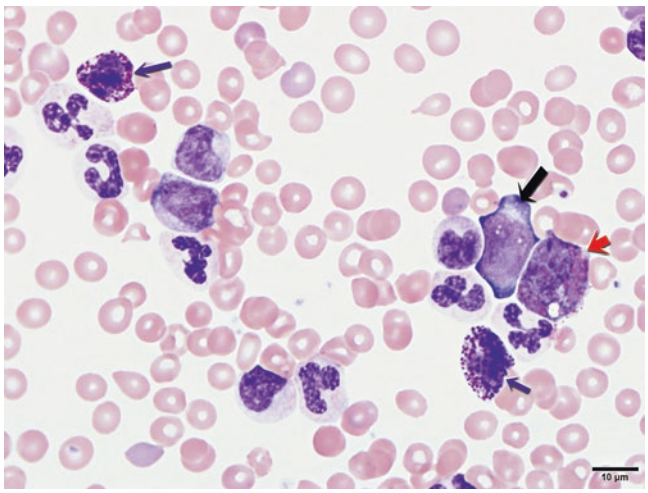

Fig. 9.9 ALL predominantly presents as de novo disease but occasionally can present as a blast crisis in patients with chronic myeloid leukemia (CML). This blood smear is from a 28-year-old man who presented with CML in chronic phase in the peripheral blood. Bone marrow biopsy revealed a blast phase with B-ALL. *BCR-ABL1* transcript is shown in Fig. 9.26

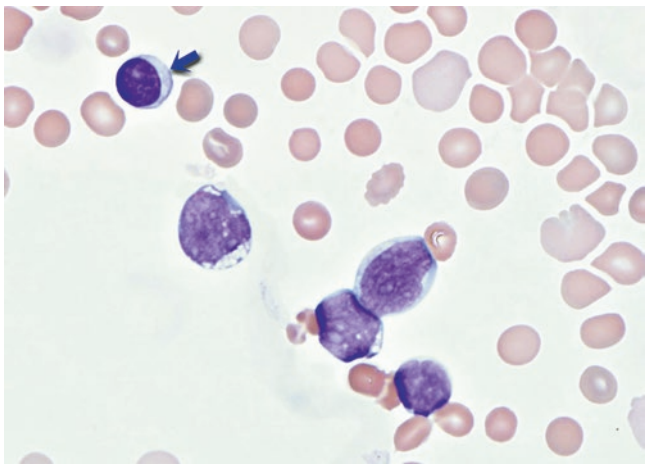

Fig. 9.11 Not infrequently, lumbar puncture may be traumatic and produce samples with peripheral blood (PB) contamination, as depicted in this image. Four blasts are present in a background of numerous red blood cells and a mature lymphocyte (blue arrow). It is not possible to distinguish whether the blasts come from PB or CSF. In this situation, a concurrent review of a PB smear is paramount to exclude a blood origin. If there are no blasts present in the PB, it is safe to assume that the blasts are from the CSF. If blasts are also present in the PB, a repeat CSF in a week or so should be recommended for further assessment

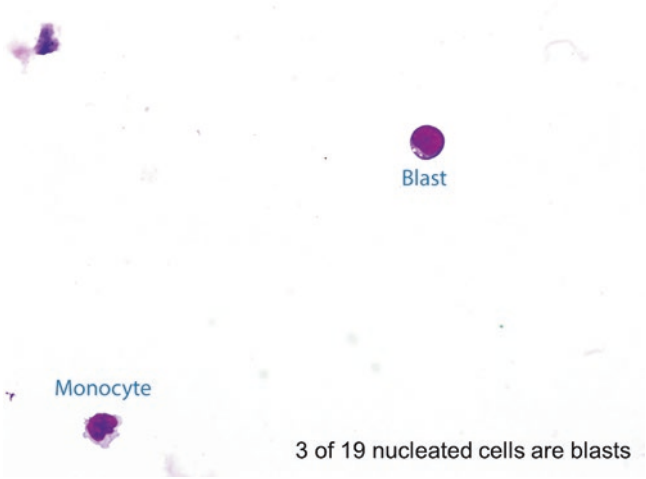

Fig. 9.10 Cerebrospinal fluid (CSF) testing is part of the standard workup for ALL (Tables 9.2 and 9.3). It is done at the time of diagnosis and periodically thereafter. A positive CSF as depicted in this image predicts an adverse prognosis. A monocyte with a moderate amount of pale cytoplasm is also seen in this image. Continuous monitoring of CSF (and testicular examination) will detect relapse of ALL, as the CNS and testes are sanctuary sites for the leukemic cells and are often the sites of relapse. Lumbar puncture also allows intrathecal delivery of chemotherapy such as methotrexate as standard of care for ALL patients

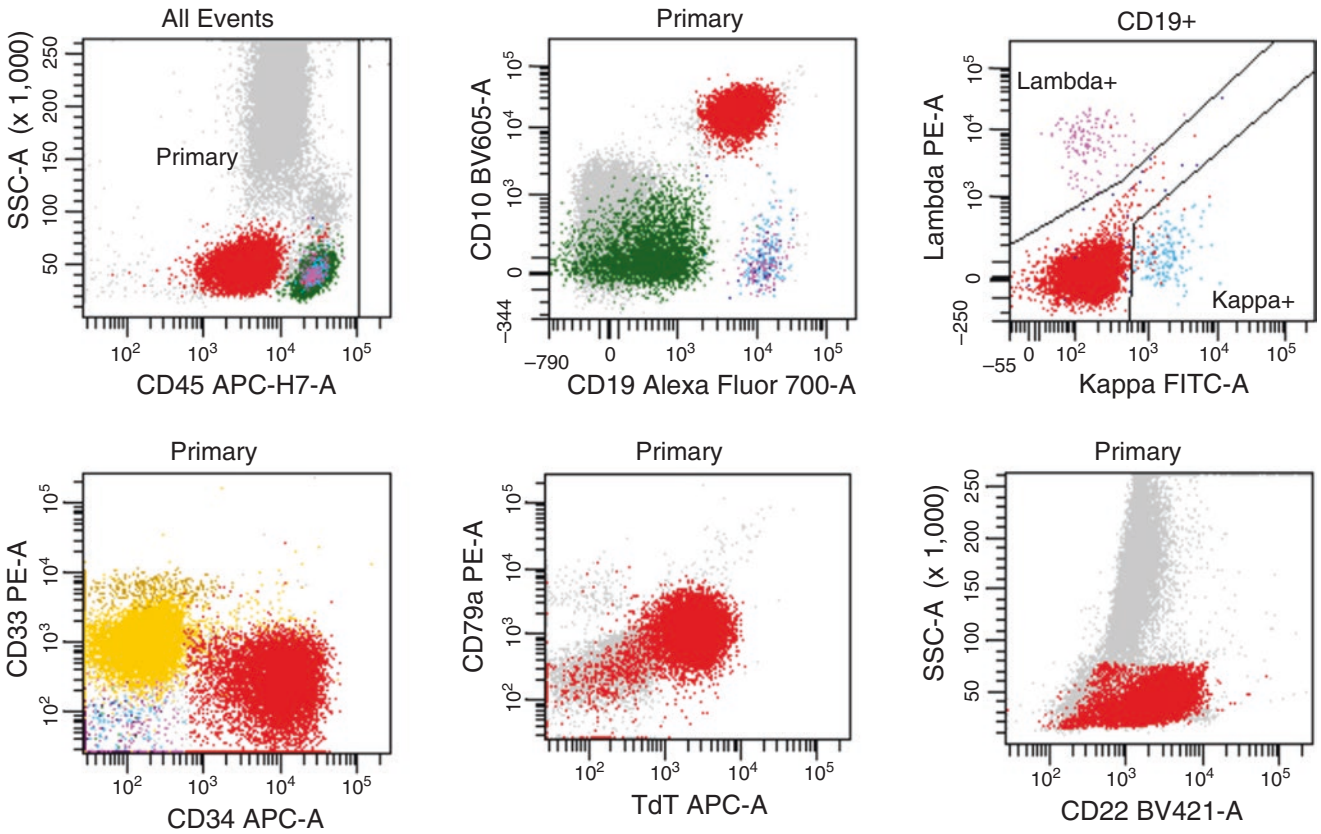

Fig. 9.12 Flow cytometric study of the blood and/or bone marrow should be performed whenever possible. Flow allows detection of six to ten antibodies simultaneously. It also allows one to detect aberrant expression of antigens with a much broader antibody panel and a sensitivity that is much superior to immunohistochemistry. It is an excellent tool for detecting minimal residual disease in the follow-up samples. ALL may arise from precursors at different maturation stages, as shown in Tables 9.4 and 9.5. Some cases of ALL have an immature immunophenotype, whereas others may exhibit mature immunophenotype. This composite flow plot illustrates a typical B-ALL flow finding, which is seen in most cases of B-ALL. The *red* population represents ALL cells that are positive for weak CD45; B-cell markers CD10, CD19, CD79a, and CD22; and immature cell markers CD34 and TdT. The blasts are negative for surface immunoglobulin light chains and the myeloid marker CD33

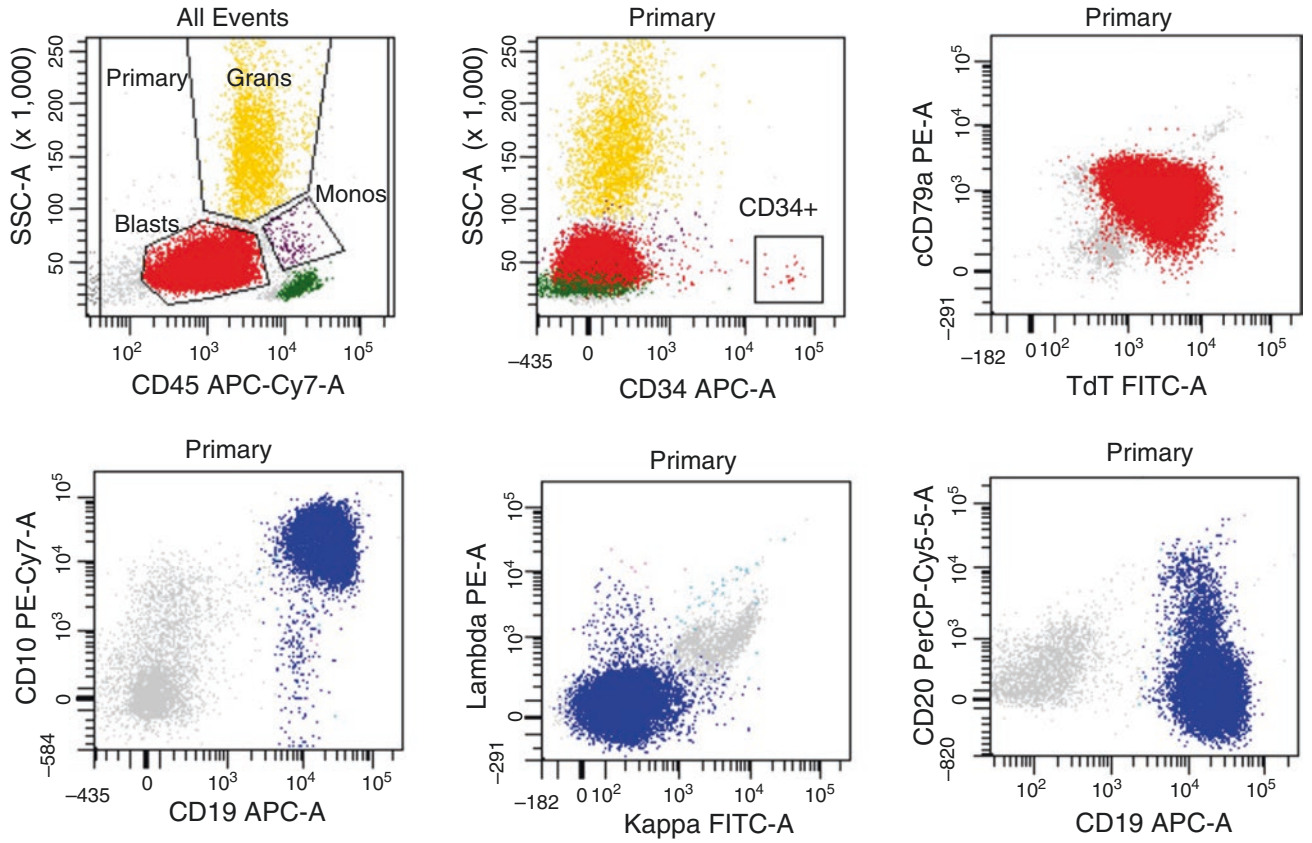

Fig. 9.13 Immunophenotype is closely associated with cytogenetic findings in certain types of ALL. Cytogenetic study is paramount in the workup of ALL, as cytogenetic abnormalities predict prognosis (Tables 9.6 and 9.7). This is an example of B-ALL with translocation (1;19) (q23;p13.3) *TCF3-PBX1*. The blast population is painted *red* on the upper panel and blue on the lower panel. Characteristically, ALLs with this translocation have a mature immunophenotype (i.e., negative for CD34). The blasts often express cytoplasmic μ chain (not done in this case) and a spectrum of CD20. The other markers expressed by the blasts include CD10, CD79a, TdT, and dim CD45. ALL with t(1;19) *TCF3-PBX1* accounts for 6% of B-ALL cases in children, but it is less common in adults. The clinical and morphologic features are indistinguishable from other types of ALL. *TCF3-PBX1* fusion has an oncologic effect. Patients with *TCF3-PBX1* ALL have an intermediate prognosis and a higher chance of CNS relapse

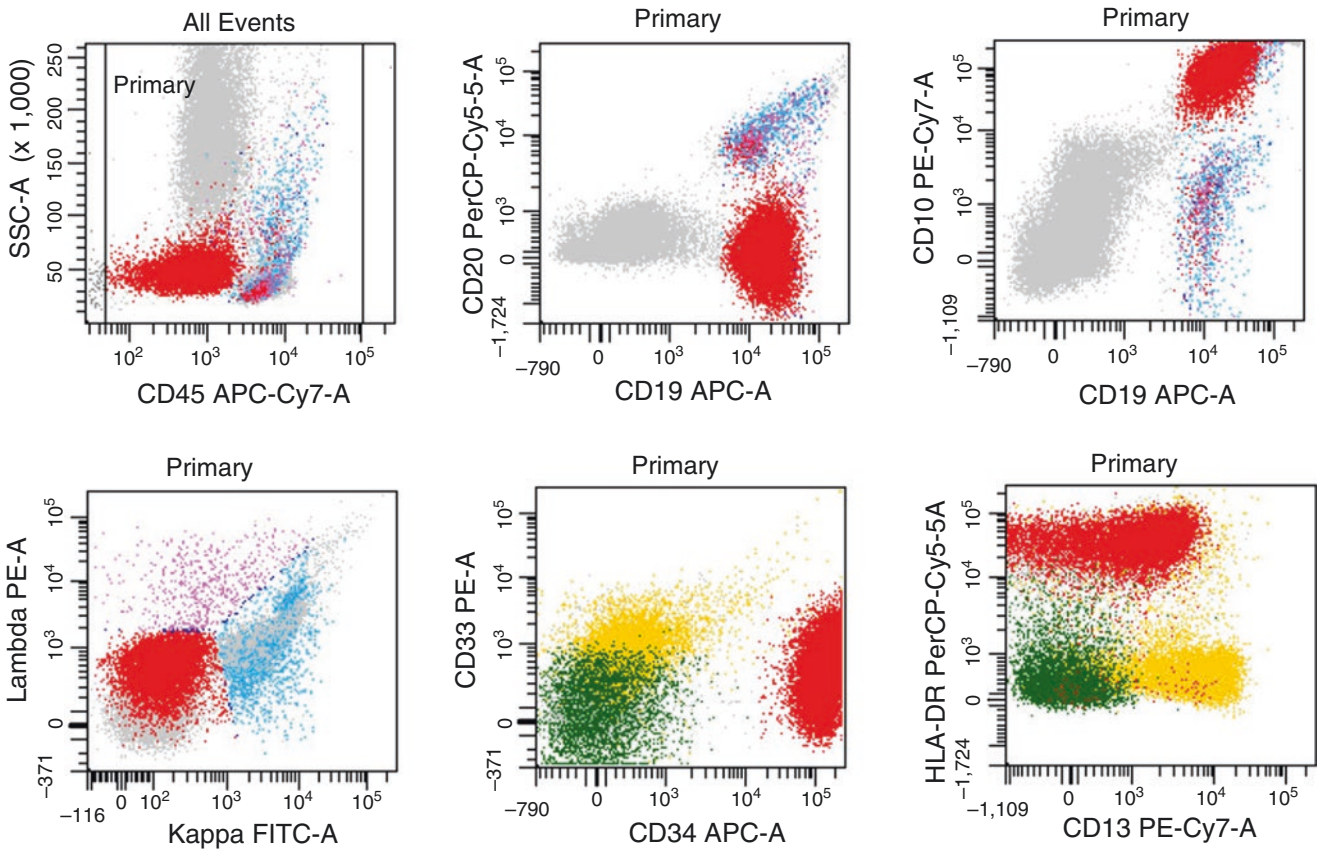

Fig. 9.14 ALL can occasionally express myeloid markers such as CD13 and CD33. This is especially prevalent in ALL with *BCR-ABL1* fusion-associated translocation 9;22 (Ph + ALL). Therefore, it is important to perform cytogenetic and/or fluorescence in situ hybridization (FISH) and/or polymerase chain reaction (PCR)-based molecular studies to exclude the translocation, as *BCR-ABL1* fusion-positive ALL carries the worst prognosis of all types of ALL. Ph + ALL accounts for 25% of adult ALL and only 2% to 4% of pediatric ALL. Most Ph + ALL cases in children produce a p190 *BCR-ABL1* fusion (see Fig. 9.27 A and B, red curve; black curve is housekeeping gene). About half of adult ALL cases produce p190 *BCR-ABL1* fusion, and the other half produce p210 *BCR-ABL1* fusion (see Fig. 9.26 A–C, green curve. The black curve is housekeeping gene. The red curve is p190 transcript, which is often seen at a low copy number at the diagnosis and often disappears after treatment). Ph + ALL tends to have hyperleukocytosis and poor response to therapy. Patients often have concurrent *IKZF1* mutation. Treatment of Ph + ALL has included a tyrosine kinase inhibitor such as imatinib, dasatinib, and nilotinib

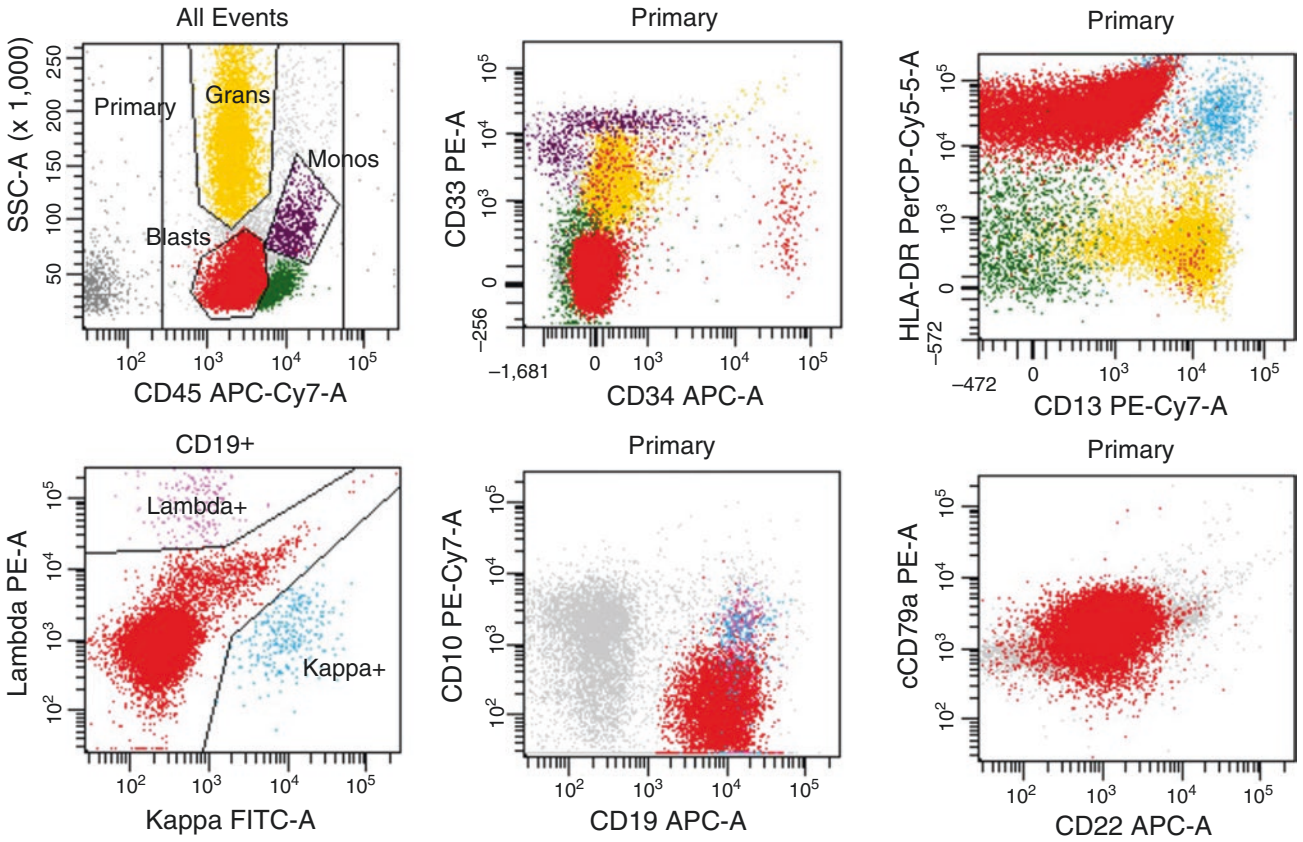

Fig. 9.15 Another type of ALL with a unique immunophenotype is ALL with *KMT2A* (i.e., *MLL*) gene rearrangement. *KMT2A* has many translocation partner genes, with t(4;11)(q21;q23) involving *AF4* and *KMT2A* genes being the most common. This translocation may occur in utero with a short latency between the translocation and the development of disease. Approximately 80% of ALLs in infants less than a year old have the *KMT2A* rearrangement. There is an increased risk of CNS involvement. The lymphoblasts are early precursors and are characteristically negative for CD10. They express CD19, CD79a, and CD22. They can also express myeloid markers such as CD13 and CD15. Leukemia with *KMT2A* translocation has a poor prognosis [11]

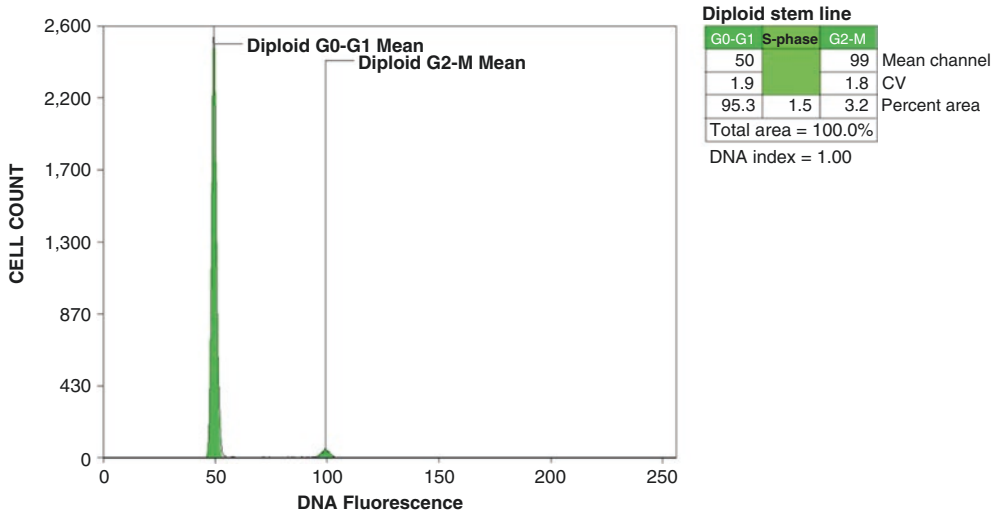

Fig. 9.16 As a routine test at the time of diagnosis, DNA index reflects the number of chromosomes in the cells (Table 9.2). This flow-based test measures DNA index with an internal diploid standard (DNA index of 1.0). As illustrated in this example, the leukemic cells are diploid, and therefore the leukemic cell peak overlaps completely with the control population; thus a single peak is seen (diploid G0-G1 mean) and the DNA index of the blasts is 1.0. The method also measures the percentages of cells in the S phase, G2 phase, and metaphase (diploid G2-M mean), although they do not have prognostic significance

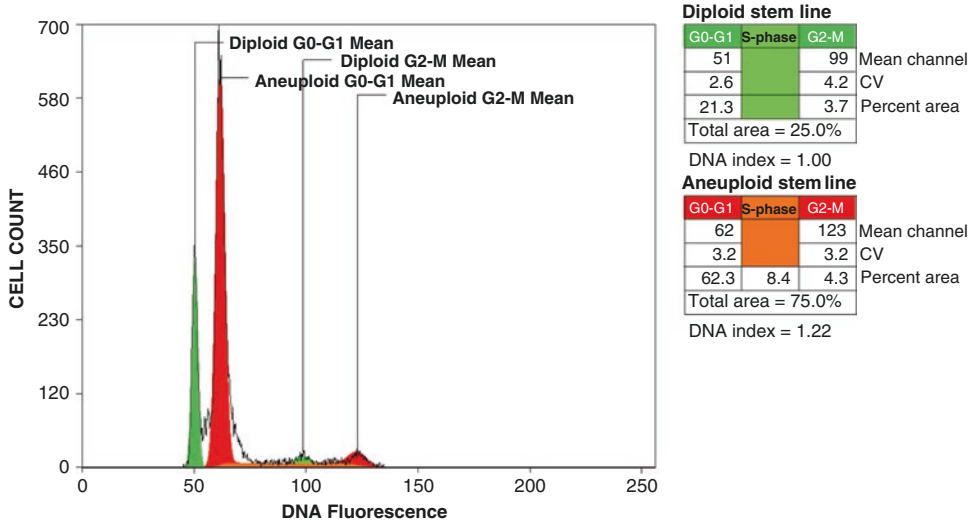

Fig. 9.17 In this DNA index study, the leukemic cells are aneuploidy with a DNA index of 1.22 (i.e., hyperdiploidy). The leukemic cell DNA content forms a separate peak (red peak, aneuploid G0-G1 mean). The diploid G0-G1 mean peak can be seen on the left as an internal control (green peak, diploid G0-G1 mean)

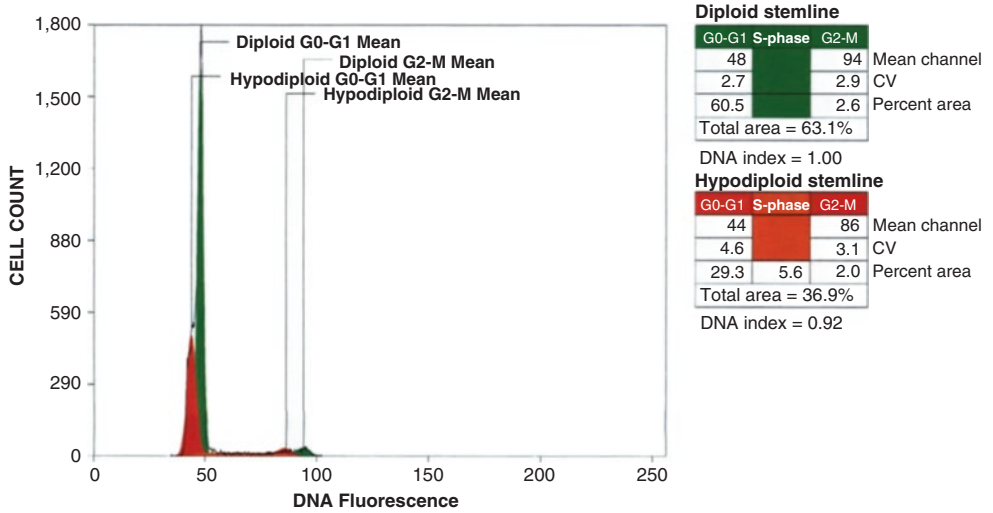

Fig. 9.18 A hypodiploid DNA index (red peak, hypodiploid G0-G1 mean) is illustrated here. The internal control diploid peak is seen on the right (green peak, diploid G0-G1 mean). The DNA index is 0.92

63~64,XY,+2,+3,+4,+5,+6,+7,+8,+10,+11,+12,+13,+14,+17,+18,+19,+21,+21,+22[cp6]/46,XY[14]

FISH reveals three copies of chromosome 4, 10, and 17

Fig. 9.19 The hyperdiploid karyotype depicted in this image (left) including triple trisomy of chromosomes 4, 10, and 17 is from a 2-year-old boy who presented with low white blood cell (WBC) count and a negative CSF; this is predictive of a good prognosis. On the right is FISH for centromeres of chromosomes 4, 10, and 17. Three copies of each chromosome (red, green, and aqua) are demonstrated here

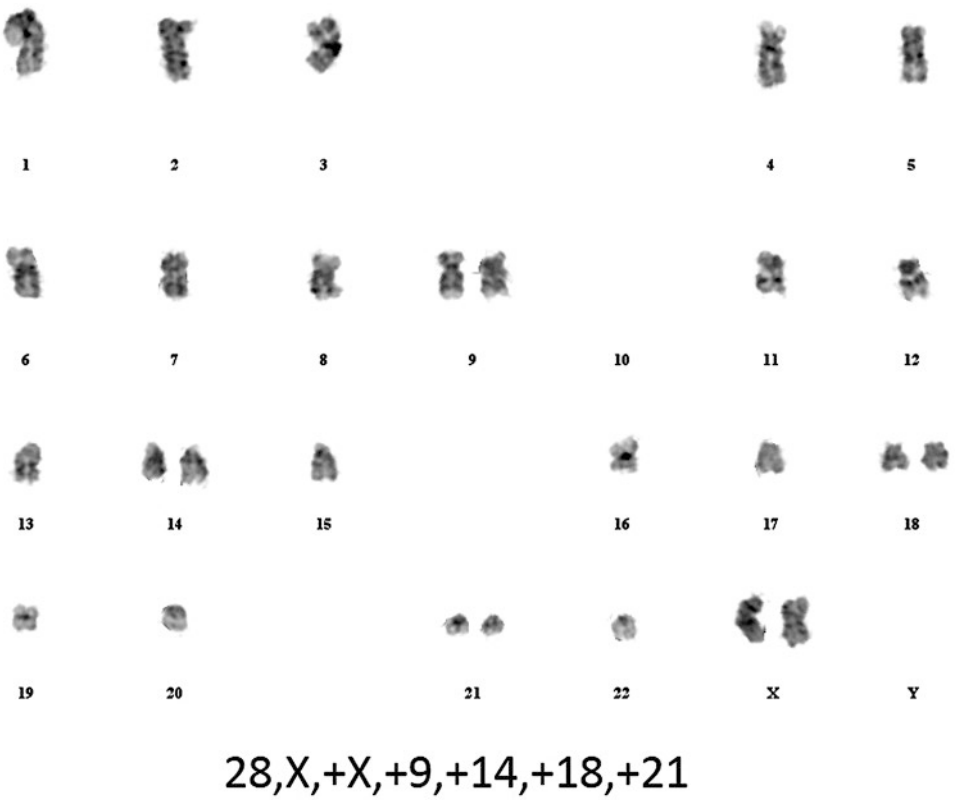

Fig. 9.20 On the contrary, this hypodiploid karyotype is indicative of a poor outcome [12]. This karyotype reveals a near-haploid cell line with two copies of chromosomes X, 9, 14, 18, and 21

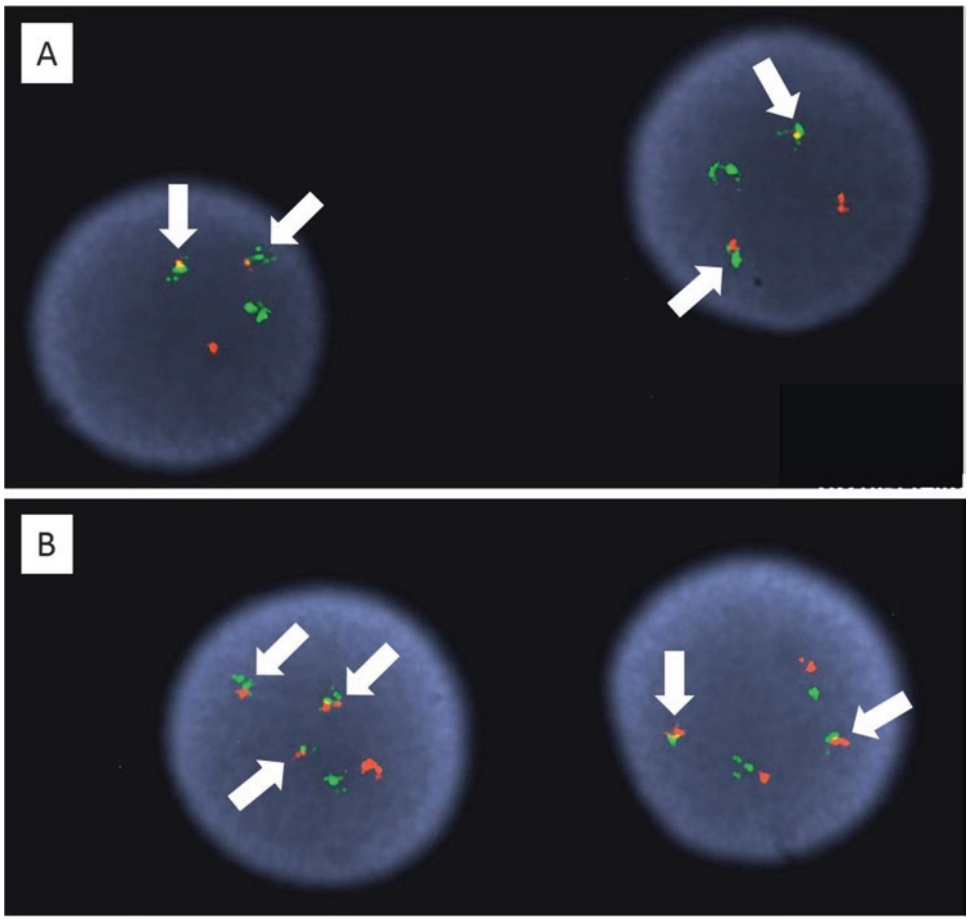

Fig. 9.21 Fluorescence in situ hybridization (FISH) is often used in conjunction with karyotype and molecular studies to identify cytogenetic abnormalities such as translocations, deletions, duplications, or chromosome numeric abnormalities. The advantage of FISH is that it can be performed on interphase cells and can detect deletions and additions that are submicroscopic on karyotype. In patients with a dry tap or when the cells fail to grow, FISH can be done on the touch preparations or direct smears. In this 48-year-old woman with ALL, conventional karyotype failed owing to a lack of growth. (**a**) FISH on the aspirate smear illustrates two copies of *BCR-ABL1* fusion (white arrows), one copy of the normal *BCR* gene (green) and one copy of normal *ABL1* (red) in the majority of the cells. (**b**) However, a small subset of cells demonstrates three fusion signals (white arrows) in the cells on the left. This finding is indicative of a clonal evolution in a minor subset of blasts

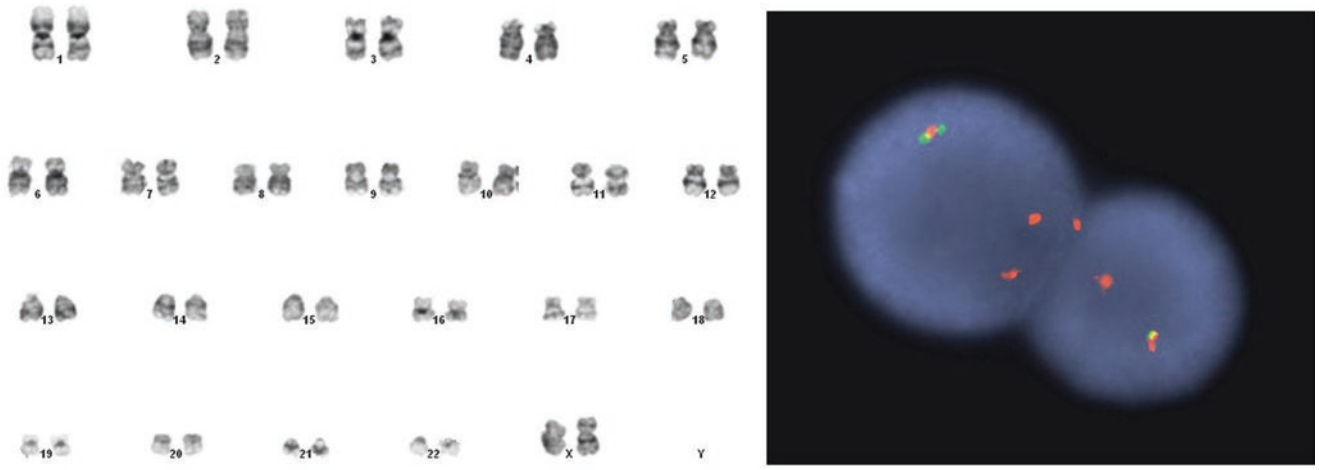

Fig. 9.22 Translocation 12;21 in ALL is regarded as a good prognostic indicator. However, this translocation is cryptic and cannot be detected by karyotype (*left*). FISH is required to establish the diagnosis (right). The t(12;21) translocation is the most common translocation in pediatric ALL, accounting for 20% of cases. It is not seen in infant ALL, and it is rare in adult ALL. The clinical and morphologic findings resemble other ALLs. Immunophenotype is similar to other ALLs, except for frequent CD13 expression. In this image, the left panel is a chromosomal study that reveals a normal karyotype 46,XX. FISH study shows an abnormal signal consistent with *ETV6/RUNX1* (i.e., *TEL/AML1*) fusion. The finding is atypical, as only one fusion signal is present. In addition, there is loss of the normal ETV6 region (no normal green signal). These atypical findings can be seen in FISH and are most likely secondary to loss of a fragment of DNA, or the remaining portion of the gene is too small for the FISH probes to hybridize. ALL with translocation of t(12;21) carries good prognosis

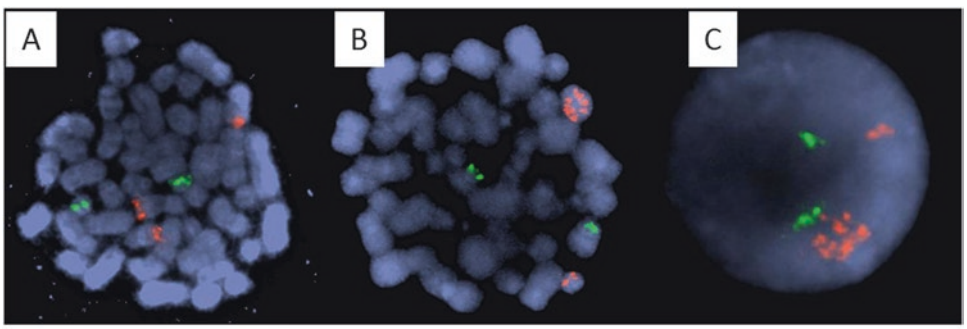

A. FISH with BCR (green) and ABL1 (red) probes on metaphase cell. B. FISH with ETV6 (green) and RUNX1 (red) probes on metaphase cell. C. FISH with ETV6 (green) and RUNX1 (red) probes on interphase cell

Fig. 9.23 Cytogenetic study in this 12-year-old girl shows a karyotype of complex abnormalities. On the Children's Oncology Group (COG) FISH panel, there are three copies of the *ABL1* gene (**a**) and multiple copies of the *RUNX1* gene (i.e., intrachromosomal amplification of the *RUNX1* gene or iAMP21) (**b**, **c**). Further workup for the *ABL1* abnormality is required, as the *ABL1* rearrangement is considered Ph-like ALL and carries a poor prognosis similar to that of Ph + ALL (Table 9.8) [13–21]. Nonetheless, this patient would be stratified as having poor prognosis based on age, complex karyotype, and iAMP21. ALL with iAMP21 tends to occur in older patients, presents with a low WBC count, and carries a poor prognosis [22]

Fig. 9.24 Patients with Down syndrome (DS) may exhibit benign hematologic abnormalities such as transient abnormal myelopoiesis in neonates and persistent macrocytosis without anemia. They also have a tenfold to 20-fold increase in the incidence of hematologic malignancies, namely, acute myeloid leukemia of megakaryocytic lineage and B-ALL. Some postulate that *RUNX1*, *CRLF2*, and/or *CBS* genes on chromosome 21 may play a role in clonal transformation in DS; others have suggested that many other genes also may be involved. B-ALL in DS is often associated with a hypodiploid karyotype and occasionally favorable karyotypes [23, 24]. DS patients with ALL usually have a good clinical outcome. These patients are particularly sensitive to chemotherapy, so appropriate dosage is important. CRLF2 abnormalities, often associated with JAK mutations, are seen in over 50% of DS-ALL (Table 9.8). Cytogenetic study on this 25-year-old man with DS shows constitutional trisomy 21 (red arrow). No other abnormality was detected

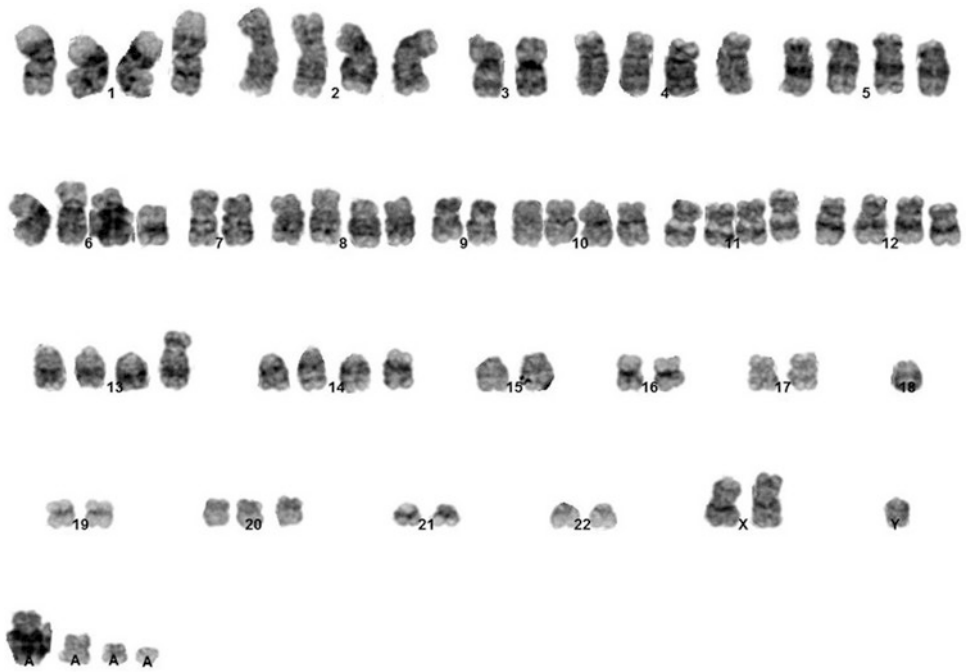

73~76<3n>,XXY,+1,+2,-3,+4,+5,+del(6)(q21),-7,+8,-9,+10,+11,add(11)(q23),add(11)(p14),+12,+13,rob(13;21)(q10;q10),+add(14)(p11.2),-15,-16,-17,-18,-19,+20,-21,-22,+2~7mar

Fig. 9.25 Occasionally, the karyotype can be highly complex, as illustrated here with 72 chromosomes. However, this is not a hyperdiploidy karyotype. On careful examination, this is a hypertriploid male chromosome complement. There are extensive structural and numerical abnormalities consisting of extra copies of chromosomes, loss of chromosomes, deletion, additional materials, a translocation, and two to seven marker chromosomes of unknown origin. This complement represents endoreduplication of a hypodiploid karyotype and predicts a poor outcome in this patient. Hypodiploid ALL tends to have a higher chance of relapse

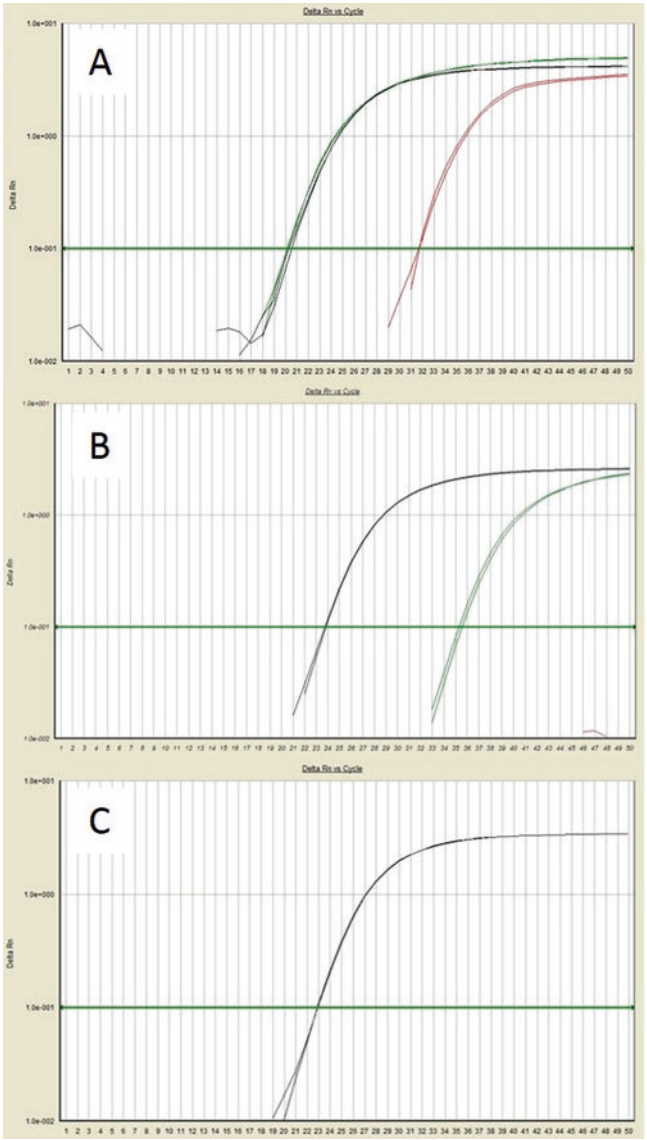

A. p210 BCR/ABL1 fusion at diagnosis

B. p210 BCR/ABL1 fusion at low level

C. BCR/ABL1 fusion negative

Fig. 9.26 In patients with Ph + ALL, the role of assessing the *BCR-ABL1* fusion transcript is not as well established as in chronic myeloid leukemia. However, data indicate that molecular response assessed by quantitative polymerase chain reaction (qPCR) is associated with outcome. Complete molecular response (CMR) is defined as the absence of detectable *BCR-ABL1* transcript with an assay sensitivity of 0.01%. Major molecular response (MMR) is defined as *BCR-ABL1*:*ABL1* ratio $\leq 0.1\%$ on the international scale (IS) for p210 *BCR-ABL1* or a three-log reduction for p190 *BCR-ABL1*, but not meeting criteria for CMR. Studies show that MMR at 3 to 6 months and sustained CMR correlates with superior survival and excellent long-term outcomes [25, 26]. In this illustration, the black curve is the transcript of the housekeeping gene *ABL1*, the green curve is the p210 *BCR-ABL1* transcript, and the red curve is the p190 *BCR-ABL1* transcript. (**a**) At the time of B-ALL diagnosis in this 48-year-old woman, a p210 *BCR-ABL1*/ABL1 transcript ratio of 0.86 is present, which indicates a high copy number of *BCR-ABL1* fusion transcript, typically seen at the time of diagnosis (green curve). Black curve is housekeeping gene, used as internal quality control. A minor product of p190 *BCR-ABL1* (red curve) at a very low level is commonly present in the background, only seen at diagnosis when the major transcript level is high; it often disappears after treatment. This transcript may represent a product of alternative splicing. (**b**) *BCR-ABL1* transcript at 3 months with a *BCR-ABL1*/ABL1 ratio of 0.00031. It fulfills the criteria for MMR, but not CMR, as there are still detectable transcripts. **C** At the 5-month mark, the patient has achieved CMR with no detectable transcript, no more green or red curves. Only the housekeeping gene (black curve) is present

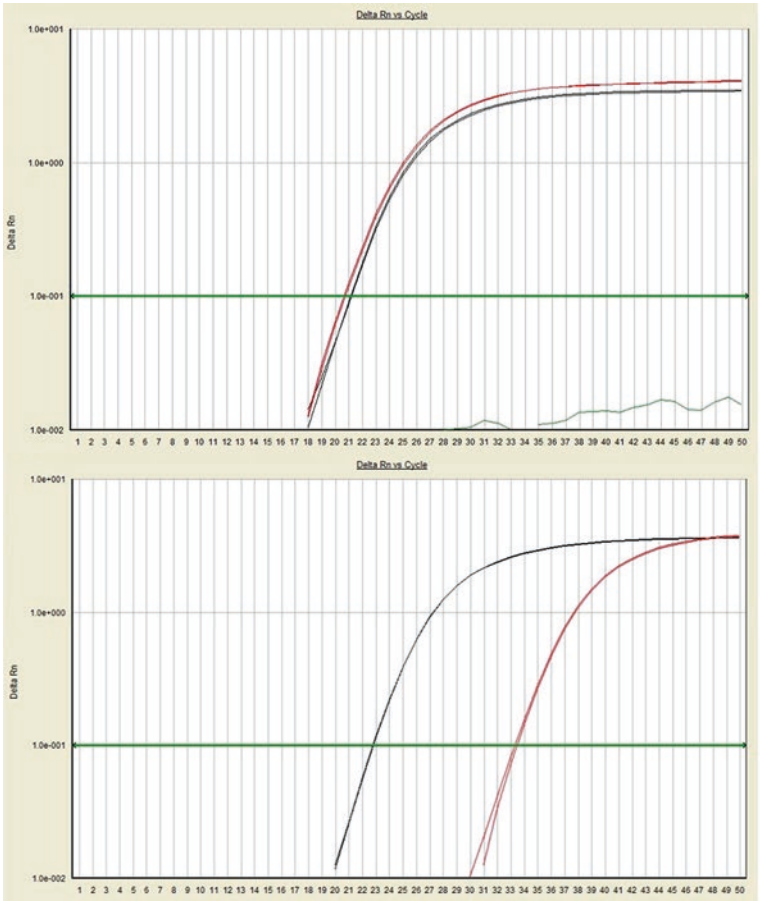

Fig. 9.27 A 13-year-old boy diagnosed with Ph ± B-ALL had a p190 *BCR-ABL1/ABL1* ratio of 1.01 (red curve), a level typically seen at diagnosis (**a**). One month later (**b**), the transcript has dropped to 0.00053, a more than three-log reduction, which meets the criteria for MMR

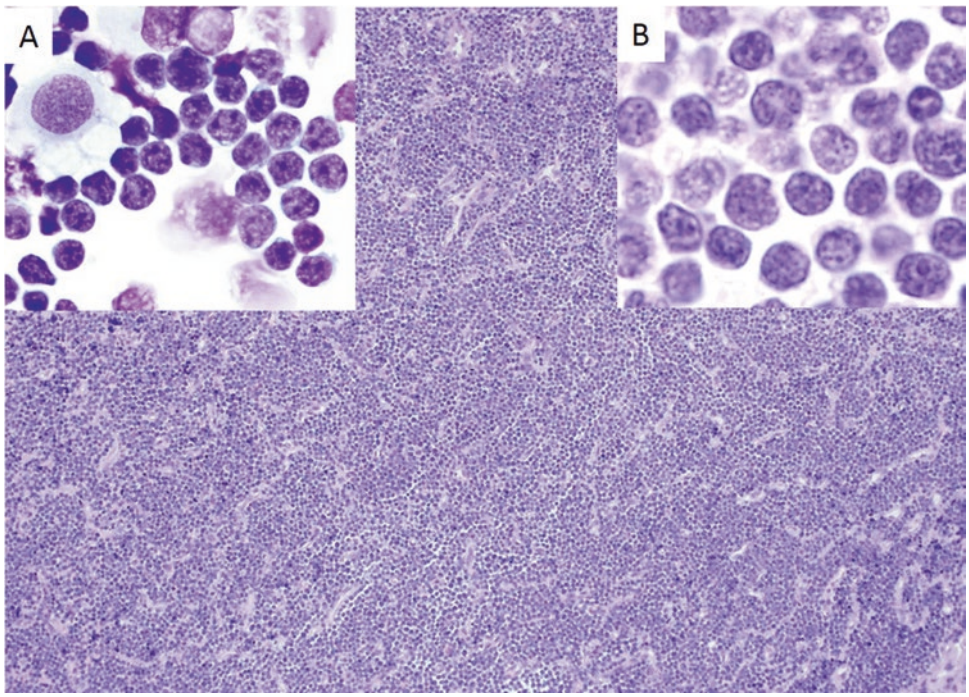

Fig. 9.28 The classic presentation of T-ALL/lymphoblastic lymphoma (LBL) is mediastinal lymphadenopathy in an adolescent or a young adult man [27, 28]. T-ALL is more common in adults, accounting for 20–25% of adult ALL. There is a male predominance, and it often presents with high WBC count, as well as lymphadenopathy, organomegaly, and an anterior mediastinal mass. The lymph node biopsy illustrated here was taken from a 15-year-old boy with a mediastinal mass and cervical lymphadenopathy, as well as pleural effusion. The low-power view exhibits a diffuse lymphoid infiltrate replacing the entire lymph node. On high power (**Inset B**), the blasts have scant cytoplasm, round to slightly irregular nuclear contours, relatively condensed to open chromatin, and occasional prominent nucleoli. On the cytospin preparation of the pleural fluid (**Inset A**), numerous blasts are seen surrounding a macrophage

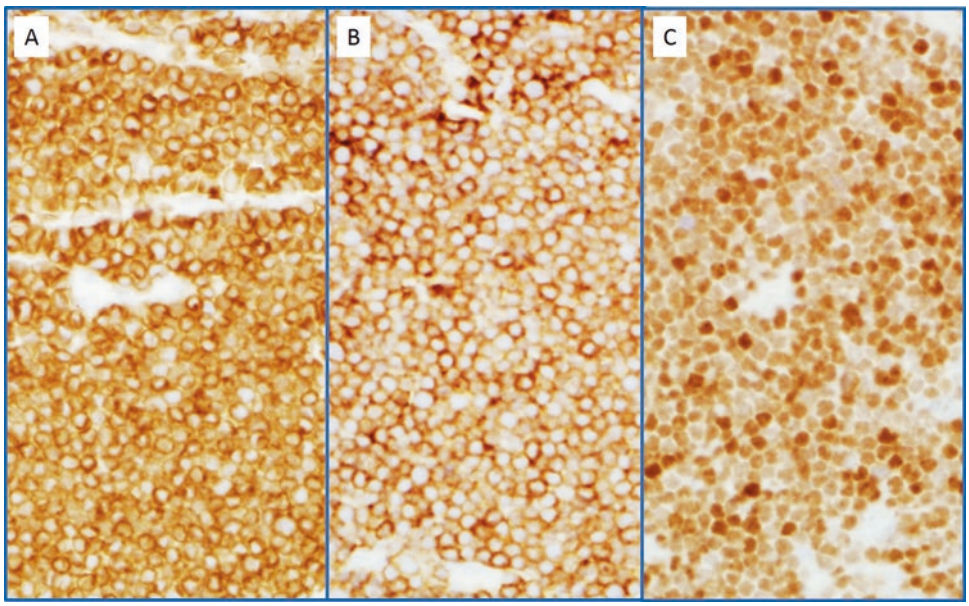

Fig. 9.29 This is the same patient as Fig. 9.28. The blasts express CD3 (**a**), TIA1 (**b**), and TdT (**c**) by immunohistochemical stains. Flow cytometric study is shown in Fig. 9.33

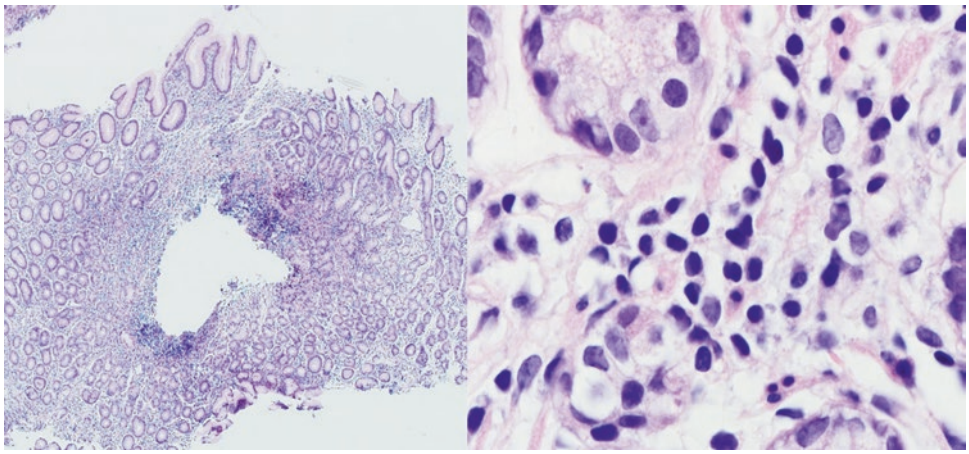

Fig. 9.30 Although T-ALL/LBL typically manifests as nodal or bone marrow disease, extranodal involvement can occur with or without mediastinal involvement. This 11-year-old boy with a history of chronic constipation presented to the emergency room with fever, vomiting, and progressing abdominal pain. Esophagogastroduodenoscopy identified multiple grape-like masses throughout the duodenum. Additional radiographic studies detected an anterior mediastinal mass. In this duodenal biopsy, there is a mild mucosal and submucosal lymphoid infiltrate (left image), which focally destroys duodenal glands, as depicted in the high-power view on the right

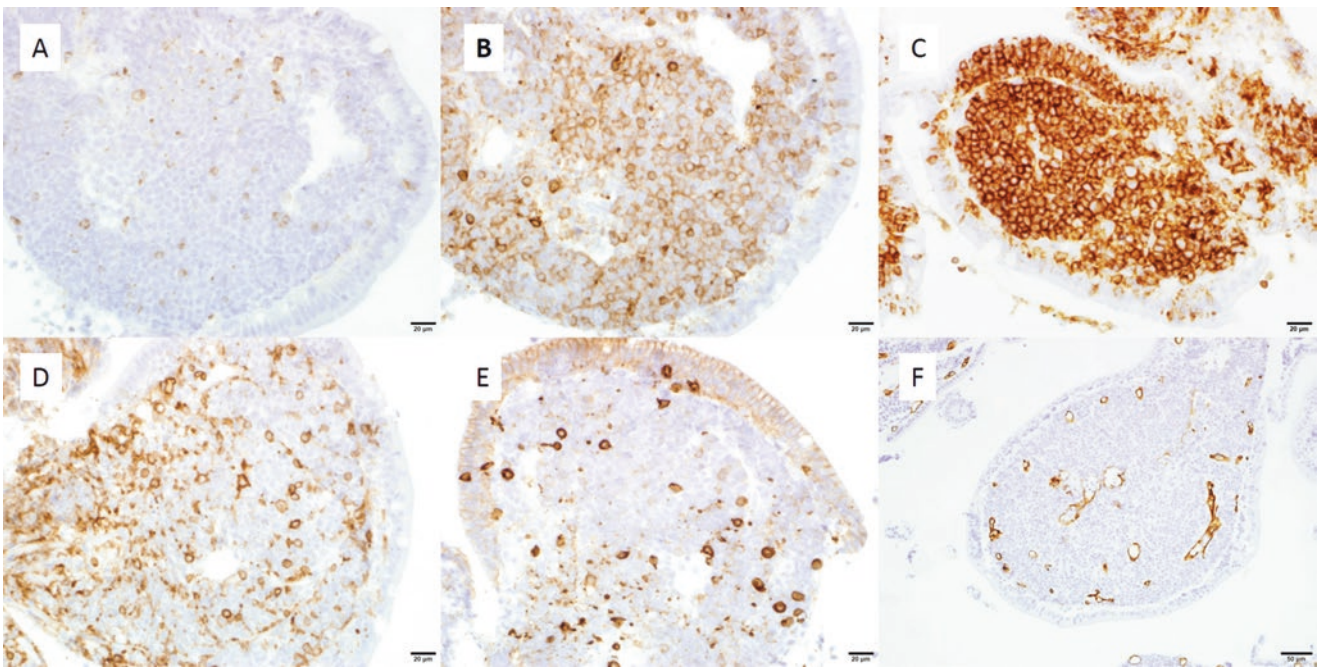

Fig. 9.31 Immunohistochemistry on the same patient as Fig. 9.30 shows that the T-ALL cells express CD3, CD5, CD7, CD43, CD45, and BCL2. They are negative for CD2, CD4, CD8, CD34, TIA, EBER, BCL6, and lysozyme. Representative immunohistochemical stains are illustrated: CD2 (**a**), CD5 (**b**), CD7 (**c**), CD4 (**d**), CD8 (**e**), and CD34 (**f**)

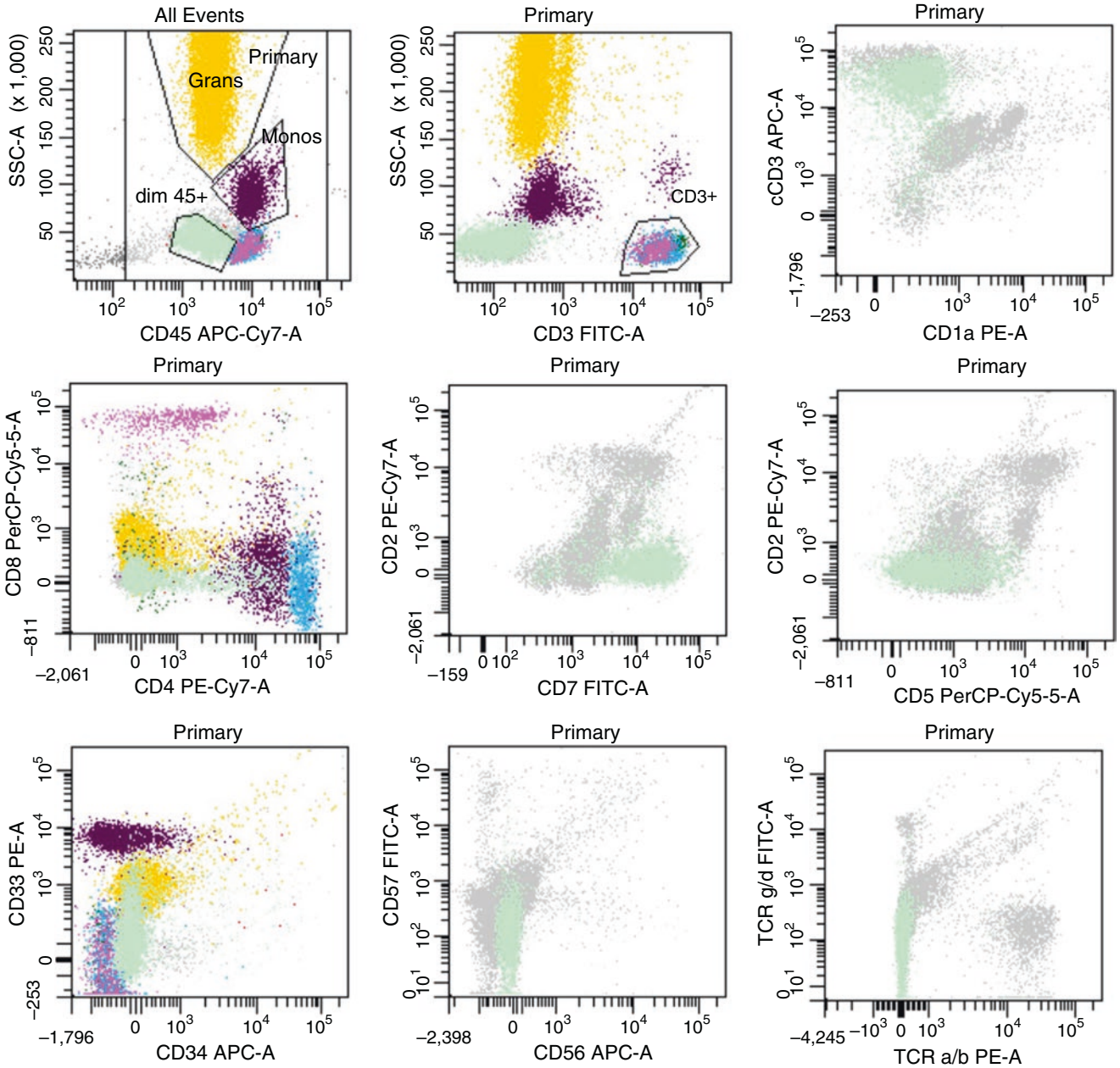

Fig. 9.32 Flow cytometry study on the peripheral blood sample from the same patient as Figs. 9.30 and 9.31 shows an abnormal population of T cells (light aquamarine), which express cytoplasmic CD3 and CD7 and are weakly positive for CD45 and a minor subset weakly positive for CD4, CD5, and CD33. They are negative for surface CD3, CD2, CD8, CD34, CD56, CD57, TCR a/b, and TCR g/d

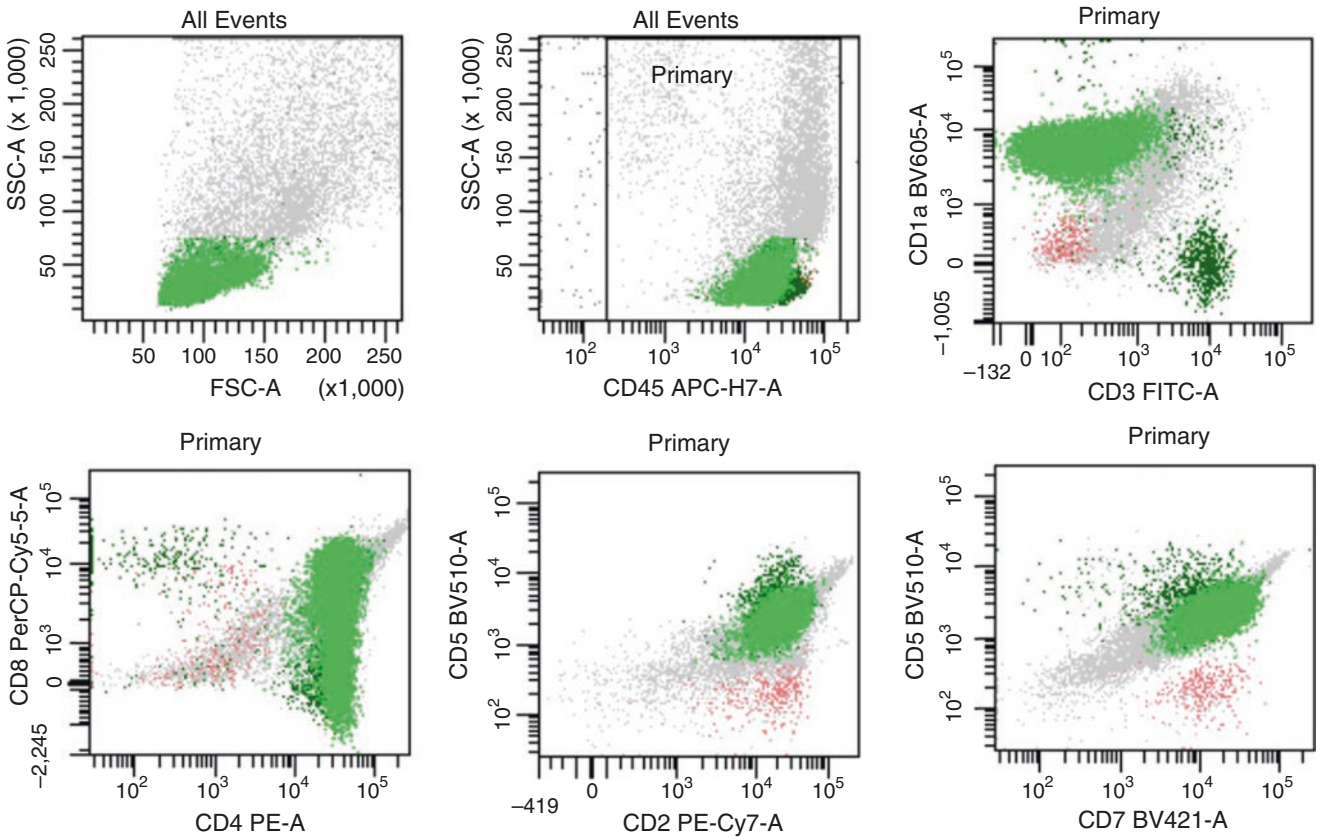

Fig. 9.33 Typical T-ALL/LBL immunophenotype, from the patient in Figs. 9.28 and 9.29, reveals that the lymphoblasts (bright green population) express CD1a, CD2, CD5, CD7, CD4, spectrum of CD8, and fairly bright CD45. They are negative for surface CD3. This immunophenotype is called "double positive" for CD4 and CD8. Along with the positive CD1a, it corresponds to the cortical thymocyte (i.e., common thymocyte) stage in T-cell development (Table 9.5)

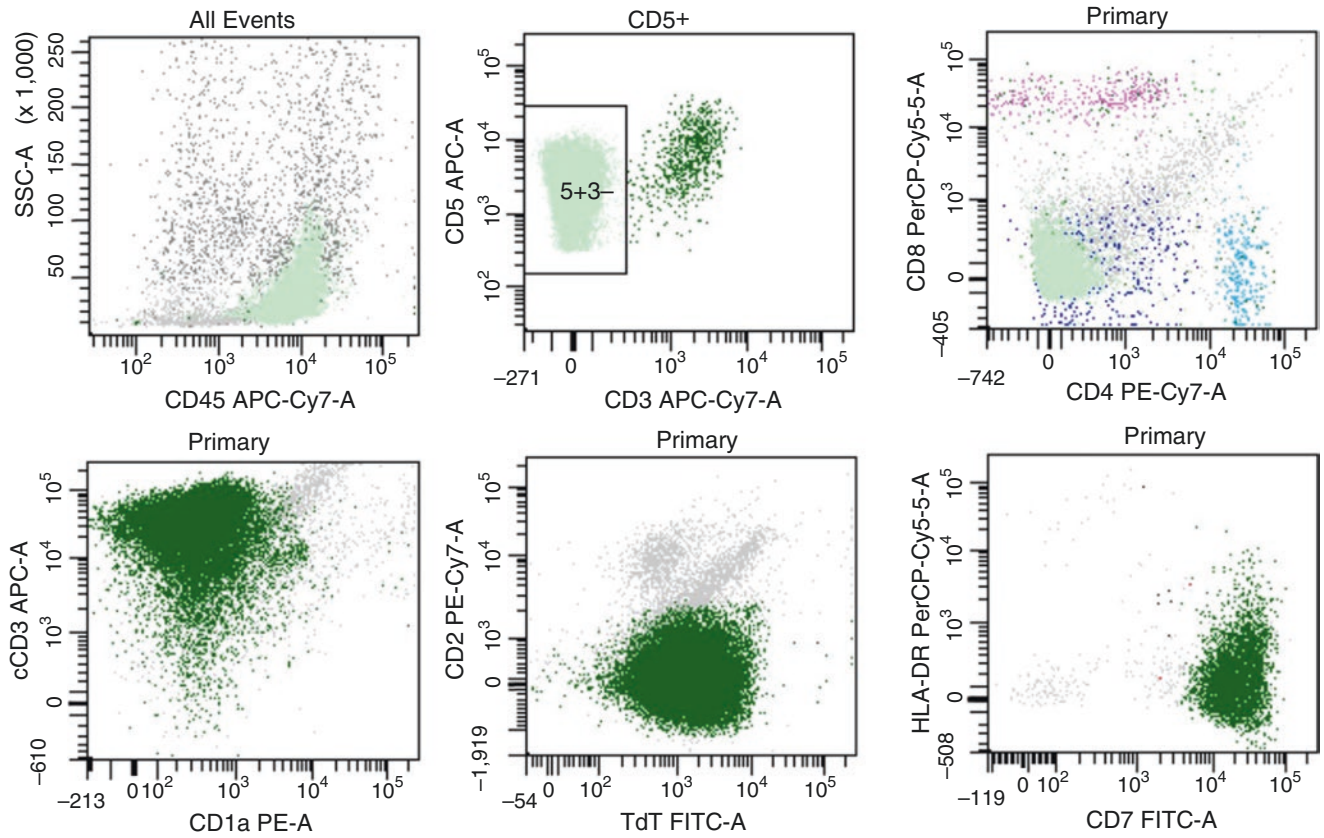

Fig. 9.34 T-ALL/LBL can exhibit a "double negative" immunophenotype. This flow cytometry panel demonstrates that the lymphoblasts (*aquamarine* on top panel, deep green on the lower panel) express CD5, CD7, cytoplasmic CD3, TdT, and CD45. They are negative for CD2, CD4, CD8, HLA-DR, and CD34 (not shown). This immunophenotype most likely represents immature thymocytes (i.e., pre-T cells) (Table 9.5)

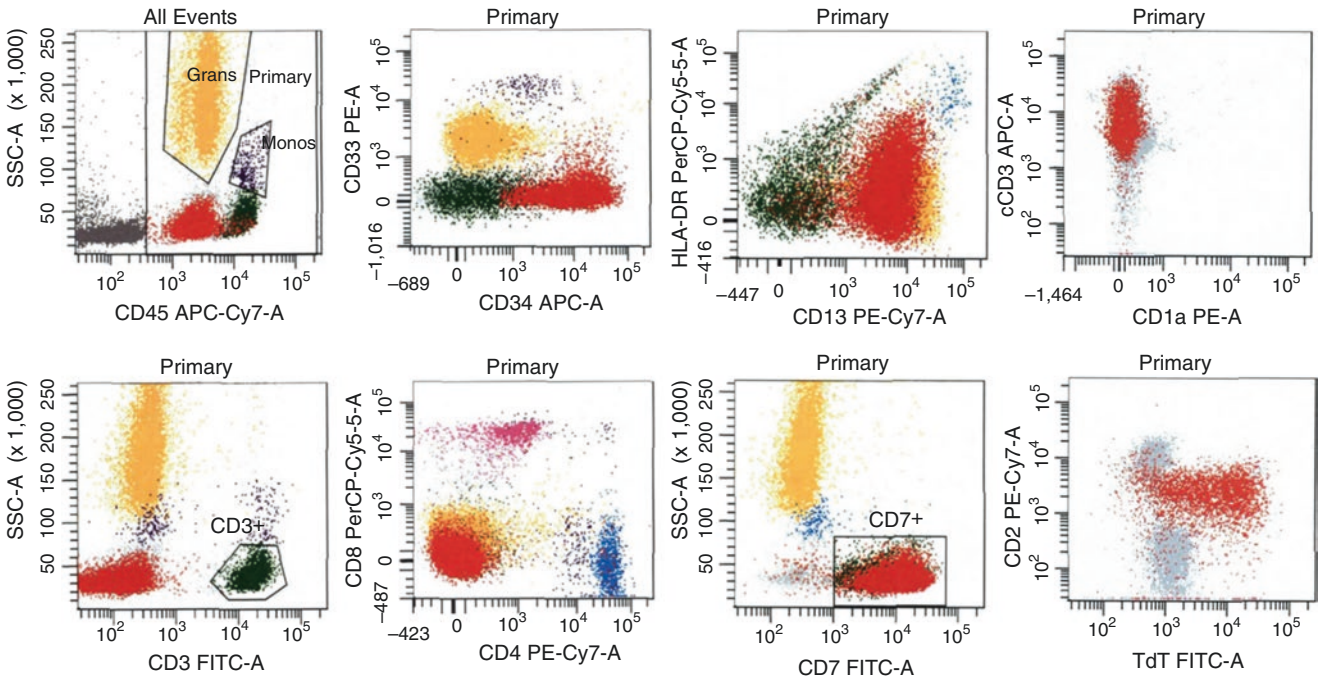

Fig. 9.35 Early T precursor (ETP) T-ALL/LBL has a unique immunophenotype and occurs in older patients. It is significant to recognize ETP T-ALL/LBL, as it carries a poor prognosis. By definition, blasts express CD7. They can also express CD2 and cytoplasmic CD3. The blasts can have CD4 but are negative for CD8. They characteristically express one or more of the myeloid or stem cell markers CD34, CD117, HLA-DR, CD13, CD33, CD11b, or CD65. This flow cytometry plot illustrates a typical finding in ETP T-ALL/LBL. The blasts are positive for CD7, CD2, cytoplasmic CD3, CD34, CD13, TdT, and subset HLA-DR. They are negative for surface CD3, CD4, CD8, and CD1a

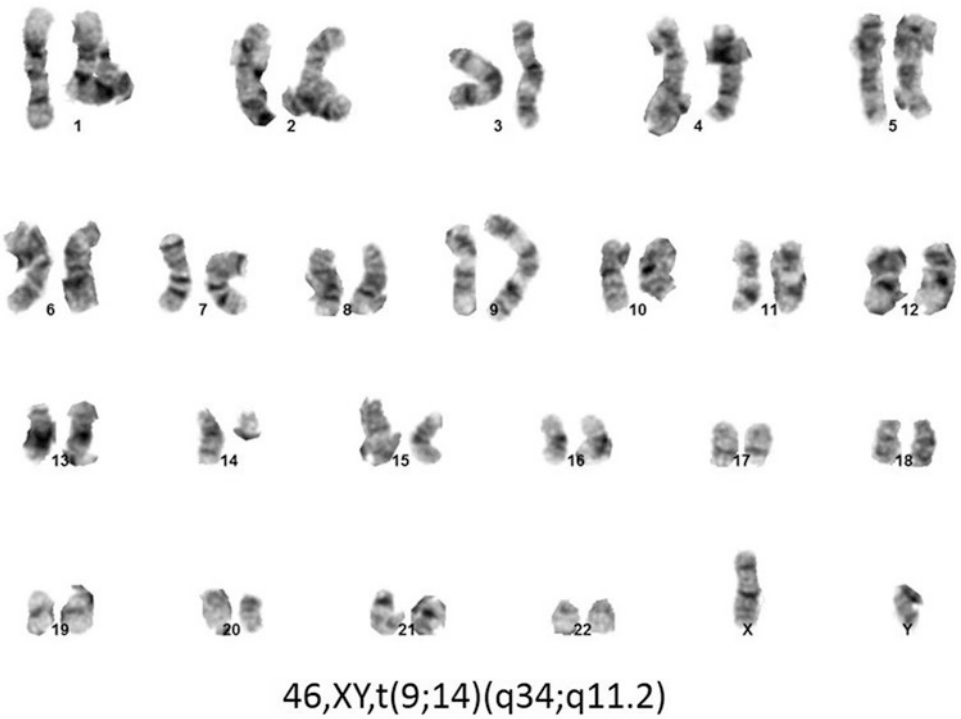

Fig. 9.36 Abnormal karyotype is found in up to 55–70% of T-ALL/LBL, including translocations and deletions [28]. The most common abnormality involves the T-cell receptor (TCR) loci (α and δ at 14q11.2, β at 7q34, and γ at 7p14), deletion of 6q, loss of 9p material through deletions or unbalanced translocations, trisomy 8, deletion of 11q, and loss of 12p (Table 9.7) [29–32]. In addition, amplifications and point mutations are commonly seen by molecular techniques. *NOTCH1* activation mutation is seen in about 50% of T-ALL and likely contributes to T-ALL pathogenesis, but it is of unknown prognostic significance [33]. *NOTCH1* encodes a transmembrane signaling protein that plays key roles in development and neoplasia. The karyotype in the image depicted is t(9;14)(q34;q11.2), *NOTCH1/TRA* (*TCR*). *NOTCH1-TRA* fusion is a rare occurrence in T-ALL [34]

Table 9.4 Clinical, pathologic, and genetic findings in B-ALL of different stages

Characteristic	Early precursor	"Common" type	Mature precursor
Clinical	Infant	Children and adults	Children, less common in adults
Pathologic finding	CD10 negative	CD10 positive	Cytoplasmic μ heavy chain, often CD34 negative
Cytogenetics	*KMT2A* (*MLL*) rearrangement	All types	t(1;19)
Prognosis	Poor	All types	Intermediate

Table 9.5 Markers expressed in T-ALL at different stages

Early T precursor (ETP)
CD7 plus one or more of the immature or myeloid markers CD34, TdT, CD117, HLA-DR, CD13
Can express cCD3 and CD2
Immature thymocyte (pre-T cell, double negative)
TdT, CD7, CD2, cCD3, variable CD34, variable HLA-DR
Common thymocyte (cortical thymocyte, double positive)
CD1a, CD2, CD5, CD7, CD4, CD8
Mature thymocyte (medullary thymocyte, either CD4 or CD8)
sCD3, CD2, CD5, CD7, CD4, or CD8

Table 9.6 Risk stratification based on clinical findings, initial laboratory tests, and cytogenetic aberrations

Characteristics	Favorable	Unfavorable
Age at diagnosis	1–10 y	<1 y or ≥10 y
Sex	Female	Male
WBC at diagnosis	$<50 \times 10^9$/L	$\geq 50 \times 10^9$/L
CNS stage	CNS1	CNS2, CNS3
Cytogenetics	Hyperdiploid > 50 chromosomes; triple trisomy of chromosomes 4, 10, and 17; t(12;21) *EVT6-RUNX1*	Hypodiploid; t(9;22) *BCR-ABL1*, *KMT2A* rearrangement, iAMP21, t(17;19) *TCF3-HLF*
Response to therapy		
Morphology	M1 at end of induction	M2, M3 at end of induction
Flow analysis	MRD < 0.1% by flow	MRD > 0.1% by flow
qPCR for *BCR-ABL1* transcript	MMR or CMR by 6 months	Did not achieve MMR by 6 months

CMR complete molecular response; *MMR* major molecular response; *MRD* minimal residual disease; *qPCR* quantitative polymerase chain reaction; *WBC* white blood cell count

Table 9.7 Common types of cytogenetic abnormalities

Abnormality	Tumor type	Frequency	Prognosis
Hyperdiploid	B-ALL	25%	Favorable
t(12;21) *ETV6-RUNX1*	B-ALL	20%	Favorable
Ph-like ALL (*BCR-ABL1*-like)	B-ALL	9%	Unfavorable
KMT2A rearrangement	B-ALL	6%	Unfavorable
t(1;19) *TCF3-PBX1*	B-ALL	4%	Intermediate
t(9;22) *BCR-ABL1*	B-ALL	3%	Unfavorable
iAMP21	B-ALL	2%	Unfavorable
Hypodiploid	B-ALL	1%	Unfavorable
Translocation *TCR* loci	T-ALL	30% of aberrant cases	Unclear
Del 6p	T-ALL	20%	Unclear
Loss of 9p	T-ALL	15%	Unclear
Trisomy 8, del11q, del12p	T-ALL	5–10%	Unclear
NUP214-ABL1 fusion	T-ALL	4–6%	Unclear
NOTCH1 activation mutation	T-ALL	50%	Unclear

TCR T-cell receptor

Table 9.8 Features of Ph-like (*BCR-ABL1*-like) ALL

Feature	Comments		
Frequency	~10% childhood ALL, ~15% high-risk ALL, 27% young adult ALL		
Characteristics	Increases with age		
	Higher WBC count at presentation		
	More common among males		
	Higher MRD at the end of induction		
	Inferior survival rate		
NGS-based test	Identifies fusions, point mutations, and expression levels from RNA input (81 genes associated with ALL, including all recurrent Ph-like ALL fusion events)		
FISH-based test	Identifies rearrangement of *CRLF2, ABL1, ABL2, PDGFRB, CSF1R, JAK2, EPOR*		
Major genes involved			
Genes	**Gene function**	**Frequency**	**Potential TKI**
CRLF2	Associated with mutant *JAK* in 50% of cases; constitutive JAK-STAT activation	<3% pediatric B-ALL	JAK inhibitor ruxolitinib
		~10% in adult ALL	
		>50% in DS-ALL	
JAK1/2	Constitutive JAK-STAT activation	Up to 35% of DS-ALL	JAK inhibitor ruxolitinib
EPOR	Constitutive JAK-STAT activation	3.9%	JAK inhibitor ruxolitinib
ABL1	*ABL* class tyrosine kinase	5% T-ALL	ABL class inhibitors: imatinib, dasatinib, nilotinib
ABL2	*ABL* class tyrosine kinase	–	ABL class inhibitors: imatinib, dasatinib, nilotinib
PDGFRB	*ABL* class tyrosine kinase	8% Ph-like ALL	ABL class inhibitors: imatinib, dasatinib, nilotinib
CSF1R	*ABL* class tyrosine kinase	–	ABL class inhibitors: imatinib, dasatinib, nilotinib
IKZF1	Kinase, a hallmark of Ph + ALL	15% pediatric ALL, 30% adult ALL, > 60% Ph + ALL	–

DS-ALL Down syndrome-associated ALL; *FISH* fluorescence in situ hybridization; *MRD* minimal residual disease; *NGS* next-generation sequencing; *TKI* tyrosine kinase inhibitor; *WBC* white blood cell

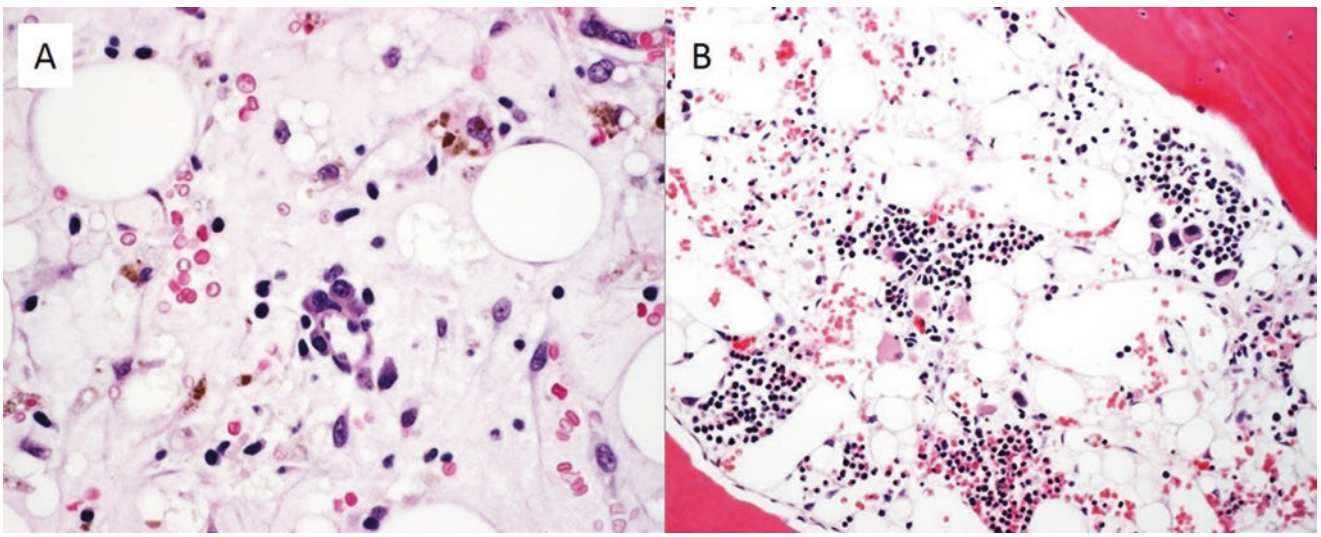

Fig. 9.37 Response to chemotherapy is significant in predicting prognosis. Early responders have superior outcome. (**a**) Bone marrow biopsy at day 14 of chemotherapy was routinely done years ago but is no longer required, given the improved sensitivity of detecting minimal residual disease (MRD) from peripheral blood by flow cytometric analysis. At day 14, the typical finding in patients responding to chemotherapy is essentially an acellular marrow with a few scattered fibroblasts, endothelial cells, plasma cells predominantly around vessels, scattered lymphocytes, and macrophages with hemosiderin pigment in a background of profound fibrinoid necrosis (chemotherapy effect). The hematopoietic cells are absent. (**b**) Bone marrow biopsy at day 29. It illustrates the beginning of bone marrow recovery, with a predominance of erythroid precursors. A few megakaryocytes can be appreciated. Myeloid lineage will soon follow

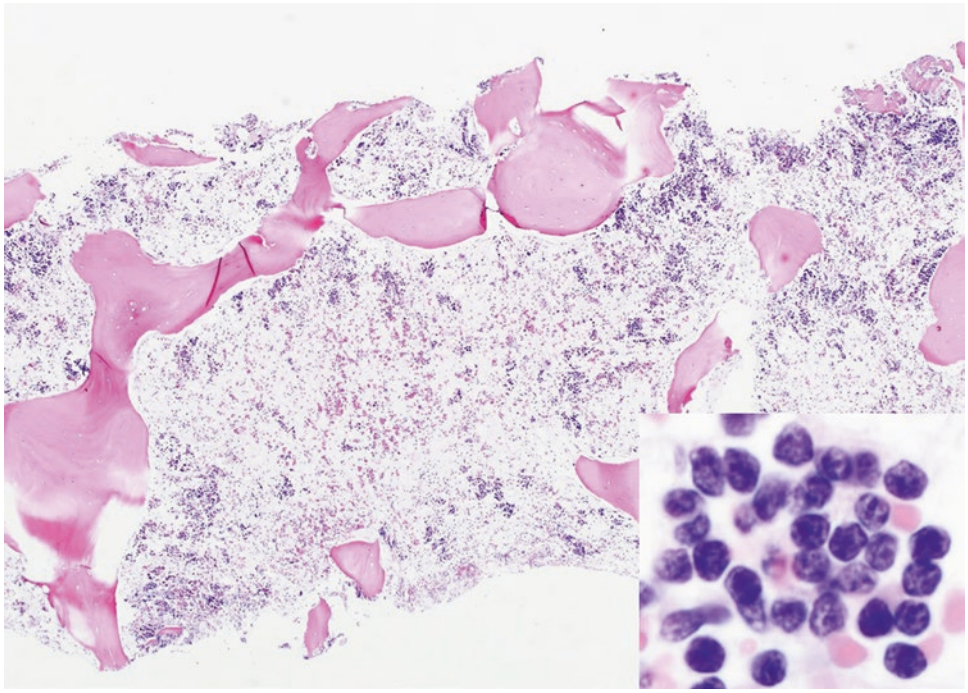

Fig. 9.38 Day 15 marrow from a 17-year-old female with residual disease. The marrow is markedly hypocellular, indicating response to chemotherapy. However, there are clusters of cells present, and on high power (**inset**), the cells are morphologically similar to the diagnostic blasts. Flow cytometric study confirms residual disease. This finding is predictive of a less favorable prognosis

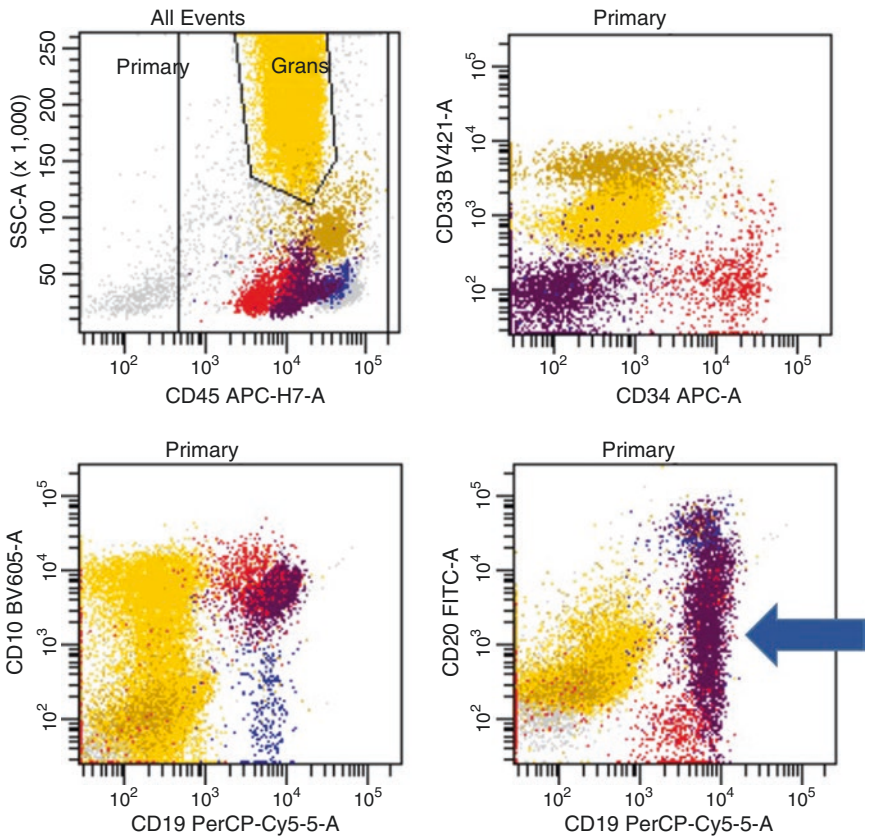

Fig. 9.39 A challenge during MRD assessment is to distinguish lymphoblasts from hematogones, which can be prominent in post-chemotherapy marrows. Lymphoblasts usually form a cluster on the flow cytometry plot. Hematogones characteristically exhibit a spectrum of maturation on CD20 expression and often loss of CD34 expression in the majority of cells. The differences between lymphoblasts and hematogones are illustrated in this composite flow plot. A 16-year-old boy diagnosed with *BCR-ABL1*-positive B-ALL experienced a slow response and eventually went into morphologic remission after 3 months of treatment. Two months after he finished his 2-year ALL protocol treatment, his BCR-ABL1 transcript started to rise. A bone marrow biopsy and flow cytometric study were performed. A population of blasts confirms relapse of his disease. The lymphoblasts form a tight cluster (red population) and express CD34, CD10, and CD19. They are negative for CD20. Hematogones (purple population) express both CD19 and CD10, but have lost CD34 expression in most cells and show a characteristic spectrum of CD20 expression (blue arrow). In contrast, the mature B cells (blue) express both CD19 and CD20, but are CD10 negative. Also seen are granulocytes (yellow) and monocytes (brown)

References

1. Swerdlow SH, Campo E, Harris NL, Jaffe ES, Pileri SA, Stein H, et al. WHO classification of tumours of haematopoietic and lymphoid tissues. 4th ed. IARC: Lyon; 2008. p. 168–78.
2. Bassan R, Maino E, Cortelazzo S. Lymphoblastic lymphoma: an updated review on biology, diagnosis, and treatment. Eur J Haematol. 2016;96:447–60. https://doi.org/10.1111/ejh.12722.
3. Moriyama T. Familial acute lymphoblastic leukemia. Rinsho Ketsueki. 2016;57:900–9. 10.11406/rinketsu.57.900.
4. Pulte D, Gondos A, Brenner H. Improvement in survival in younger patients with acute lymphoblastic leukemia from the 1980s to the early 21st century. Blood. 2009;113:1408–11. https://doi.org/10.1182/blood-2008-06-164863.
5. Pui CH, Mullighan CG, Evans WE, Relling MV. Pediatric acute lymphoblastic leukemia: where are we going and how do we get there? Blood. 2012;120:1165–74. https://doi.org/10.1182/blood-2012-05-378943.
6. Madhusoodhan PP, Carroll WL, Bhatla T. Progress and prospects in pediatric leukemia. Curr Probl Pediatr Adolesc Health Care. 2016;46:229–41. https://doi.org/10.1016/j.cppeds.2016.04.003.
7. Sorensen JT, Gerald K, Bodensteiner D, Holmes FF. Effect of age on survival in acute leukemia. 1950-1990. Cancer. 1993;72:1602–6.
8. Irken G, Oren H, Gülen H, Duman M, Uçar C, Atabay B, et al. Treatment outcome of adolescents with acute lymphoblastic leukemia. Ann Hematol. 2002;81:641–5.
9. Jacobson S, Tedder M, Eggert J. Adult acute lymphoblastic leukemia: a genetic overview and application to clinical practice. Clin J Oncol Nurs. 2016;20:E147–54.
10. Paul S, Kantarjian H, Jabbour EJ. Adult acute lymphoblastic leukemia. Mayo Clin Proc. 2016;91:1645–66. https://doi.org/10.1016/j.mayocp.2016.09.010.
11. Guest EM, Stam RW. Updates in the biology and therapy for infant acute lymphoblastic leukemia. Curr Opin Pediatr. 2017;29:20–6. https://doi.org/10.1097/MOP.0000000000000437.
12. Safavi S, Paulsson K. Near-haploid and low-hypodiploid acute lymphoblastic leukemia: two distinct subtypes with consistently poor prognosis. Blood. 2017;129:420–3. https://doi.org/10.1182/blood-2016-10-743765.
13. Bhojwani D, Kang H, Menezes RX, Yang W, Sather H, Moskowitz NP, *et al.*; Children's Oncology Group Study; Dutch Childhood Oncology Group; German Cooperative Study Group for Childhood Acute Lymphoblastic Leukemia. Gene expression signatures predictive of early response and outcome in high-risk childhood acute lymphoblastic leukemia: a Children's Oncology Group Study [corrected]. J Clin Oncol 2008;26:4376–4384. doi: https://doi.org/10.1200/JCO.2007.14.4519
14. Moorman AV, Schwab C, Ensor HM, Russell LJ, Morrison H, Jones L, et al. IGH@ translocations, CRLF2 deregulation, and microdeletions in adolescents and adults with acute lymphoblastic leukemia. J Clin Oncol. 2012;30:3100–8. https://doi.org/10.1200/JCO.2011.40.3907.
15. Roberts KG, Morin RD, Zhang J, Hirst M, Zhao Y, Su X, et al. Genetic alterations activating kinase and cytokine receptor signaling in high-risk acute lymphoblastic leukemia. Cancer Cell. 2012;22:153–66. https://doi.org/10.1016/j.ccr.2012.06.005.
16. Mullighan CG. The genomic landscape of acute lymphoblastic leukemia in children and young adults. Hematology Am Soc Hematol Educ Program. 2014;2014(1):174–80. https://doi.org/10.1182/asheducation-2014.1.174.
17. Roberts KG, Li Y, Payne-Turner D, Harvey RC, Yang YL, Pei D, et al. Targetable kinase-activating lesions in Ph-like acute lymphoblastic leukemia. N Engl J Med. 2014;371:1005–15. https://doi.org/10.1056/NEJMoa1403088.
18. Boer JM, Steeghs EM, Marchante JR, Boeree A, Beaudoin JJ, Beverloo HB, et al. Tyrosine kinase fusion genes in pediatric BCR-ABL1-like acute lymphoblastic leukemia. Oncotarget. 2017;8:4618–28. 10.18632/oncotarget.13492.
19. Den Boer ML, van Slegtenhorst M, De Menezes RX, Cheok MH, Buijs-Gladdines JG, Peters ST, et al. A subtype of childhood acute lymphoblastic leukaemia with poor treatment outcome: a genome-wide classification study. Lancet Oncol. 2009;10:125–34. https://doi.org/10.1016/S1470-2045(08)70339-5.
20. Jain N, Roberts KG, Jabbour E, Patel K, Eterovic AK, Chen K, et al. Ph-like acute lymphoblastic leukemia: a high-risk subtype in adults. Blood. 2017;129:572–81. https://doi.org/10.1182/blood-2016-07-726588.
21. Roberts KG, Gu Z, Payne-Turner D, McCastlain K, Harvey RC, Chen IM, et al. High frequency and poor outcome of Philadelphia chromosome–like acute lymphoblastic leukemia in adults. J Clin Oncol. 2017;35:394–401. https://doi.org/10.1200/JCO.2016.69.0073.
22. Ryan SL, Matheson E, Grossmann V, Sinclair P, Bashton M, Schwab C, et al. The role of the RAS pathway in iAMP21-ALL. Leukemia. 2016;30:1824–31. https://doi.org/10.1038/leu.2016.80.
23. Buitenkamp TD, Izraeli S, Zimmermann M, Forestier E, Heerema NA. van den Heuvel-Eibrink MM, *et al.* Acute lymphoblastic leukemia in children with Down syndrome: a retrospective analysis from the Ponte di Legno study group. Blood. 2014;123:70–7. https://doi.org/10.1182/blood-2013-06-509463.
24. Lee P, Bhansali R, Izraeli S, Hijiya N, Crispino JD. The biology, pathogenesis and clinical aspects of acute lymphoblastic leukemia in children with Down syndrome. Leukemia. 2016;30:1816–23. https://doi.org/10.1038/leu.2016.164.
25. Zhang L, Ramjit RT, Hill CE, Arellano M, Khoury HJ, Mann KP. Clinical significance of quantitative monitoring and mutational analysis of *BCR-ABL1* transcript in Philadelphia chromosome positive B lymphoblastic leukemia. Leuk Lymphoma. 2015;57:364–9. https://doi.org/10.3109/10428194.2014.1003059.
26. Short NJ, Jabbour E, Sasaki K, Patel K, O'Brien SM, Cortes JE, et al. Impact of complete molecular response on survival in patients with Philadelphia chromosome–positive acute lymphoblastic leukemia. Blood. 2016;128:504–7. https://doi.org/10.1182/blood-2016-03-707562.
27. Belver L, Ferrando A. The genetics and mechanisms of T cell acute lymphoblastic leukaemia. Nat Rev Cancer. 2016;16:494–507. https://doi.org/10.1038/nrc.2016.63.
28. Karrman K, Johansson B. Pediatric T-cell acute lymphoblastic leukemia. Genes Chromosomes Cancer. 2017;56:89–116. https://doi.org/10.1002/gcc.22416.
29. Heerema NA, Sather HN, Sensel MG, Kraft P, Nachman JB, Steinherz PG, et al. Frequency and clinical significance of cytogenetic abnormalities in pediatric T-lineage acute lymphoblastic leukemia: a report from the Children's Cancer Group. J Clin Oncol. 1998;16:1270–8.
30. Schneider NR, Carroll AJ, Shuster JJ, Pullen DJ, Link MP, Borowitz MJ, et al. New recurring cytogenetic abnormalities and association of blast cell karyotypes with prognosis in childhood T-cell acute lymphoblastic leukemia: a pediatric oncology group report of 343 cases. Blood. 2000;96:2543–9.
31. Karrman K, Forestier E, Heyman M, Andersen MK, Autio K, Blennow E, et al. Clinical and cytogenetic features of a population-based consecutive series of 285 pediatric T-cell acute lymphoblastic leukemias: rare T-cell receptor gene rearrangements are associated with poor outcome. Genes Chromosomes Cancer. 2009;48:795–805. https://doi.org/10.1002/gcc.20684.

32. Girardi T, Vicente C, Cools J, De Keersmaecker K. The genetics and molecular biology of T-ALL. Blood. 2017;129:1113–23. https://doi.org/10.1182/blood-2016-10-706465.
33. Reichard K. Precursor B- and T-cell acute lymphoblastic leukemia/lymphoma (aka lymphoblastic leukemia/lymphoma). In: Foucar K, Reichard K, Czuchlewski D, editors. Bone marrow pathology. 3rd ed. Chicago: ASCP; 2010. p. 591–615.
34. Suzuki S, Nagel S, Schneider B, Chen S, Kaufmann M, Uozumi K, et al. A second NOTCH1 chromosome rearrangement: t(9;14)(q34.3;q11.2) in T-cell neoplasia. Leukemia. 2009;23:1003–6. https://doi.org/10.1038/leu.2008.366.